

GEOMETRIC TRANSFORMATION FOR DOUBLE HELICAL WIRE RODS

A THESIS SUBMITTED TO THE GRADUATE DIVISION OF THE UNIVERSITY
OF HAWAII IN PARTIAL FULFILLMENT OF THE
REQUIREMENTS FOR THE DEGREE OF

MASTER OF SCIENCE

IN

MECHANICAL ENGINEERING

DECEMBER 2004

By

Manuel Munoz Hardy

Thesis Committee:
Ronald H. Knapp, Chairperson
Ko Moe Htun
Ian Robertson

ACKNOWLEDGMENTS

The author of this research wishes to express his most sincere appreciation to Professor Ronald H. Knapp for his support, patience and encouragement during this effort. Dr. Knapp provided all the necessary support and guidance needed to achieve the results obtained in this research, key issues for succeeding in class and especially in this thesis. Also the author wishes to express the most sincere acknowledgments to Professors Ko Moe Htun and Ian N. Robertson for serving as members of the committee, providing important support and advise as well.

The author also gratefully acknowledges the financial support provided by the Mechanical Engineering Department as well as Ms. Min Zhong (fellow graduate student), for her camaraderie and assistance with important topics during my stay at UH.

TABLE OF CONTENTS

Acknowledgments.....	iii
List of Figures	vi
CHAPTER 1: INTRODUCTION	1
1.1 Background	1
1.1.1 Wire Rope	1
1.1.2 The Double Helical Cross-Section.....	2
1.1.3 Mathematical Tools Used to Develop the Model	3
1.2 Research Objective	3
CHAPTER 2: DESCRIPTION OF THE MATHEMATICAL TOOLS	4
2.1 Pencil of Circles and Theory of Envelopes.....	4
2.2 Equation of Pencil of Spheres and Theory of Envelopes.....	5
CHAPTER 3: APPLICATION TO SINGLE HELICAL WIRE RODS.....	9
3.1 Description of the Model	9
3.2 Helical Centerline and Pencil of Spheres.....	10
3.3 Application of Theory of Envelopes.....	11
3.4 Intersection Between Circles and Plane $z=0$	13
3.5 Relationship Between the Covering Angle and the Helix Angle.....	15
3.6 Final Representation of the Helical Wire Rod Cross-Section.....	17
CHAPTER 4: APPLICATION TO DOUBLE HELICAL ROUND WIRES.....	18
4.1 Three-Dimensional Coordinate System for Double Helix.....	19
4.2 Second Helix Centerline and Transformation to a Global Coordinate System	21
4.3 Coordinates of the Second Helix in the Global Coordinate System $x-y-z$	26
4.4 Application of Pencil of Spheres Equation and Theory of Envelopes to Double Helix Centerline	27
4.5 Intersecting the Circle with a Plane Parallel to Plane $x-y$	29
4.6 Mathematical Arrangement Used when Two Helix Have Opposite Direction	31
CHAPTER 5: NUMERICAL SOLUTION.....	33

5.1	Relationship Between First Rotational Angle, θ , and Second Rotational Angle, ϕ	33
5.2	Numerical Analysis to Obtain the Resultant Transverse Cross-Section for Double Helical Wire Rods	34
5.3	Considering More Than One Wire.....	35
5.4	Flow Chart for Numerical Analysis	36
CHAPTER 6: VERIFICATION OF THE MODEL		40
6.1	Internal Shapes of the Double Helix Wire Rods and the Contact Points with Outside Bean and Inside Bean	40
6.2	Verification and Comparison with a Physical Model	41
CHAPTER 7: CONCLUSIONS		49
REFERENCES.....		51

LIST OF FIGURES

<u>Figure</u>	<u>Page</u>
1-1 Double-helical rope.....	2
2-1 Equation of circles	4
2-2 Mathematical basis for describing the cam profile by means of the theory of envelopes is shown.....	5
2-3 Some sphere over the path	6
2-4 Resultant Circles from the intersection between the sphere and the plane.....	7
2-5 Circle perpendicular to the path	7
2-6 Envelope of the “Pencil of the Spheres”	8
3-1 Coordinates of the centerline helical path.....	11
3-2 Intersection between circles and plane $z=0$	12
3-3 Intersection between one circle and plane parallel to the cable cross-section.....	13
3-4 Cross-section of the helical wire rod	15
3-5 Piece of helical wire rod shows the relationship between the covering angle, θ , and the helix angle, α	16
4-1 Convention sign used in the model.....	18
4-2 Coordinate system for double helical wire rods.....	20
4-3 Top view of the second helical wire rod.....	21
4-4 Coordinated of the second helix in the local coordinate system represented by the axes x_s, y_s	22
4-5 First coordinate transformation.....	23
4-6 Second coordinate transformation about z_s axis.....	24
4-7 Coordinates of the second helix centerline when two helix angles are opposite in direction.....	31
5-1 Relationship between θ and α	33
5-2 Double helical wire rod cable with seven strands.....	34
5-3 Nomenclature used in double helical wire rods	35
5-4 Considering more than one wire in the strand	36

5-5	Flow chart for numerical solution.....	38
5-6	One complete strand in the double helical cross-section	39
6-1	Points of intersection between outside bean, inside bean and internal shapes.....	41
6-2	Strand cross-section	42
6-3	Double helical wire rod cross-section with two helix angles having same direction	43
6-4	Double helical wire rod cross-section with two helix angles having opposite direction	44
6-5	The two possible cross-section for a double helical wire rod with some physical characteristic.....	45
6-6	Physical model for a double helical wire rod.....	46
6-7	Cross-section of a physical model	47
6-8	Two model with same physical characteristic but with wire's center in different position	48

CHAPTER 1

INTRODUCTION

1.1 Background

1.1.1 Wire Rope

High strength wire ropes, are very important tensile structural members. Due to their flexibility and high strength, ropes are in widespread use throughout the mechanical, civil, electrical and ocean engineer industries. Applications include lifts, electrical power transmission, aircraft arresting cables, suspension bridges, and anchoring or moving of marine vessels.

A wire rope is an assembly of steel wires or other materials that are helically-served around a core that results in a flexible metallic cord capable of resisting high tensile loads.

A steel wire rope has three basic components that vary in complexity according to specific applications. These components include:

1. Strands (wire rods helically-served around a straight core wire)
2. Straight Core Unit (wire or strand)
3. Rope (strand helically-served around a straight core unit)

Round wires are the basic building units of a wire rope. They are laid around a center in a specific pattern, in one or more layers, to form what is called 'strand'. A group of strands laid around a straight 'core' forms a wire rope.

Because of its double-helical geometry the wire rope exhibits very high bending flexibility and large internal damping. Also the service life of double-helical rope construction is considerably greater than a single-helical construction. Figure 1.1 is a schematic representation of a double-helical rope construction. The strands around the center core lie on a helical path, and the wires in these strands also are helically-laid around a core wire.

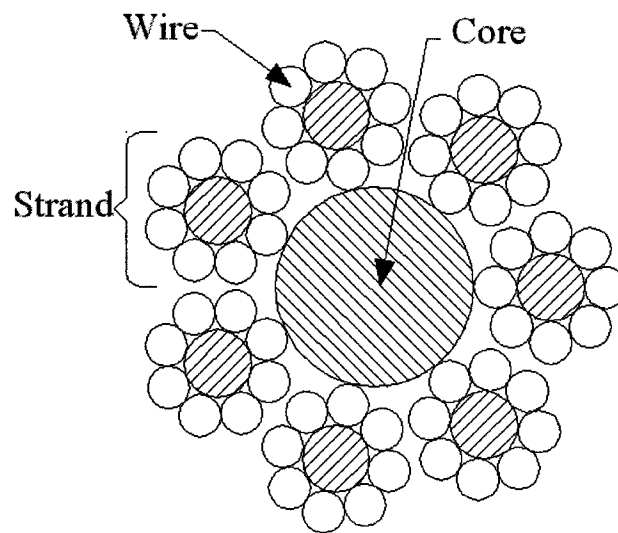


Figure 1-1 Double-helical rope

1.1.2 The Double Helical Cross-Section

The true shape of a double-helical geometry in a rope cross-section is needed for the design of ropes to predict the interstitial voids that need to be filled with water-blocking material. Commercially-available software such as AutoCAD, Inventor, Ideas, Mechanical Desktop, etc. are unable to develop this geometry. Thus, the objective of this study is to develop the parametric equations needed to produce scaled rope cross-section plots.

1.1.3 Mathematical Tools Used to Develop the Model

Two fundamental mathematical tools are used to describe the cross-section of helical wire rods. The premier tool is the equation of the “Pencil of Spheres” where coordinates of the second helix centerline in a global coordinate system is found. To establish the centerline, coordinates of the helical path geometric transformations are developed. The equation of the “Pencil of Spheres” for the second helix is then intersected with a plane perpendicular to the rope axis. This results in the true shape of the helical round rods.

1.2 Research Objective

The objective of this research is to derive a mathematical model that describes the exact geometry of double-helical round rods in a plane perpendicular to the rope axis. Using this model, a computer program is developed to plot the rope cross-section to a true scale.

CHAPTER 2

DESCRIPTION OF THE MATHEMATICAL TOOLS

2.1 Pencil of Circles and Theory of Envelopes

A circle of radius, R , with its center at the origin of plane x - y is represented by the equation

$$x^2 + y^2 = R^2 \quad (2.1)$$

If the center of this circle is moved to the coordinates x_0, y_0 , the equation that represents this circle becomes

$$(x - x_0)^2 + (y - y_0)^2 = R^2 \quad (2.2)$$

Figure 2.1 represent this schematically. Now if some path connecting the centers of a number of such circles in the plane is known, an envelope as seen in Figure 2.2 is formed. If the derivative of every circle equation is taken with respect to some parameter defining circle movement along the path, a curve normal to the path and envelope is formed.

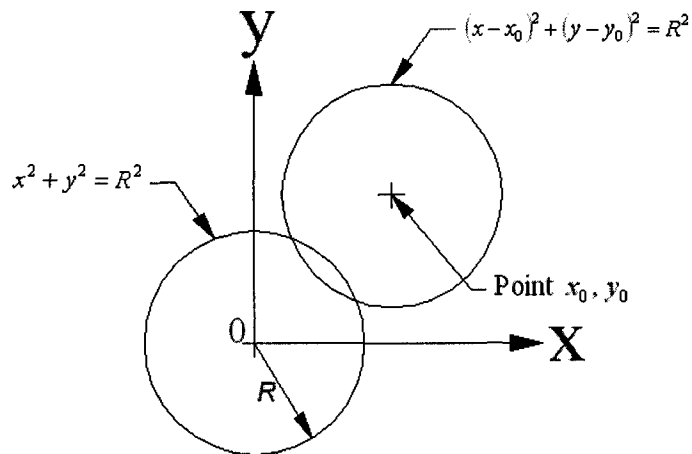


Figure 2-1 Equation of circles

The intersection of this curve with the circle defines points on the envelope.

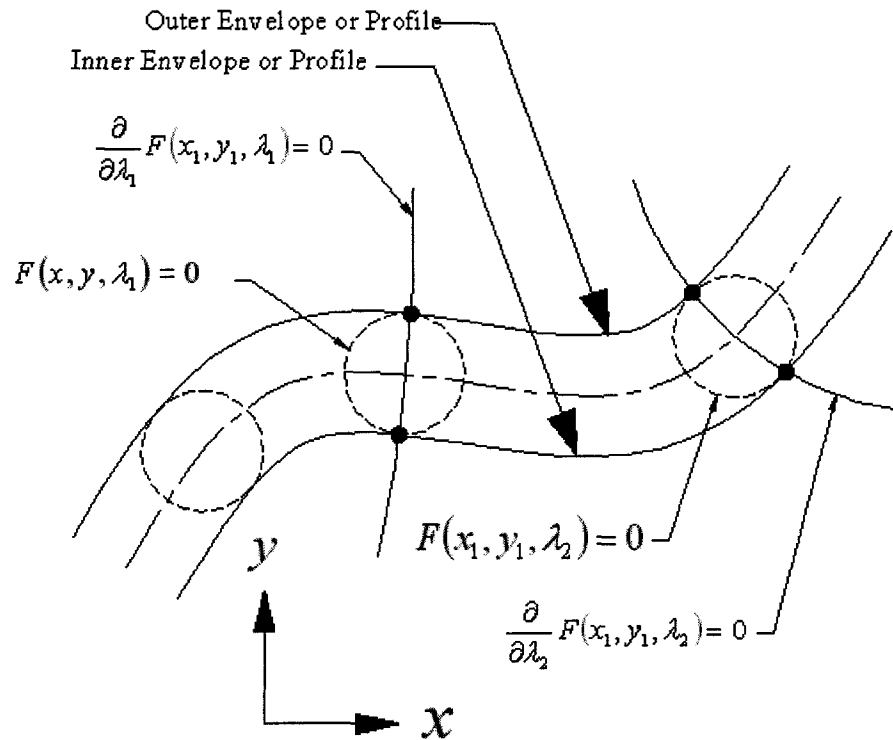


Figure 2-2 Mathematical basis for describing the cam profile by means of the theory of envelopes is shown

2.2 Equation of Pencil of Spheres and Theory of Envelopes

By using the equation of the spheres instead of the equation of the circles, the theory of envelopes can be developed in three-dimensional space.

A sphere with its center laying in the origin of some coordinate system x-y-z, is represented by

$$x^2 + y^2 + z^2 = R^2 \quad (2.3)$$

Where R = spherical radius. If the center of the sphere is moved to the coordinates x_0, y_0, z_0 , the equation becomes

$$(x - x_0)^2 + (y - y_0)^2 + (z - z_0)^2 = R^2 \quad (2.4)$$

Now if the center of the sphere is moved over some curved path in space, the intersection between of “Pencil of Spheres” and the derivative of this equation with respect to the parameters that describe the position of this sphere in space equal to zero will define an envelope that can be intersected with a plane perpendicular to the rope axis. This intersection will provide the true shape of the helical rods in the rope transverse cross-section.

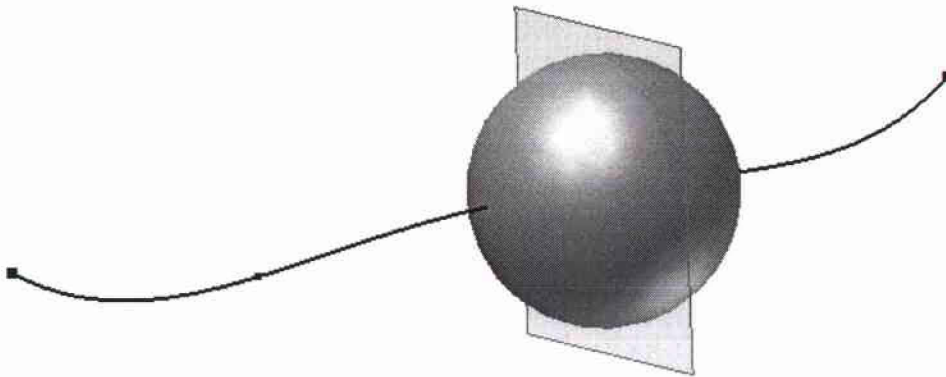


Figure 2-3 Some sphere over the path

Figure 2.3 shows a sphere whose center follows a curved path. Taking the derivative of the spherical equation with respect to the coordinates of the center of the sphere results in a plane equation that is perpendicular to the path of motion. This is illustrated in Figure 2.4. The intersection of this plane with the sphere results in the circle depicted in Figure 2.5. Movement of this circle along the curved path forms the equation of the envelope of the “Pencil of Spheres”.

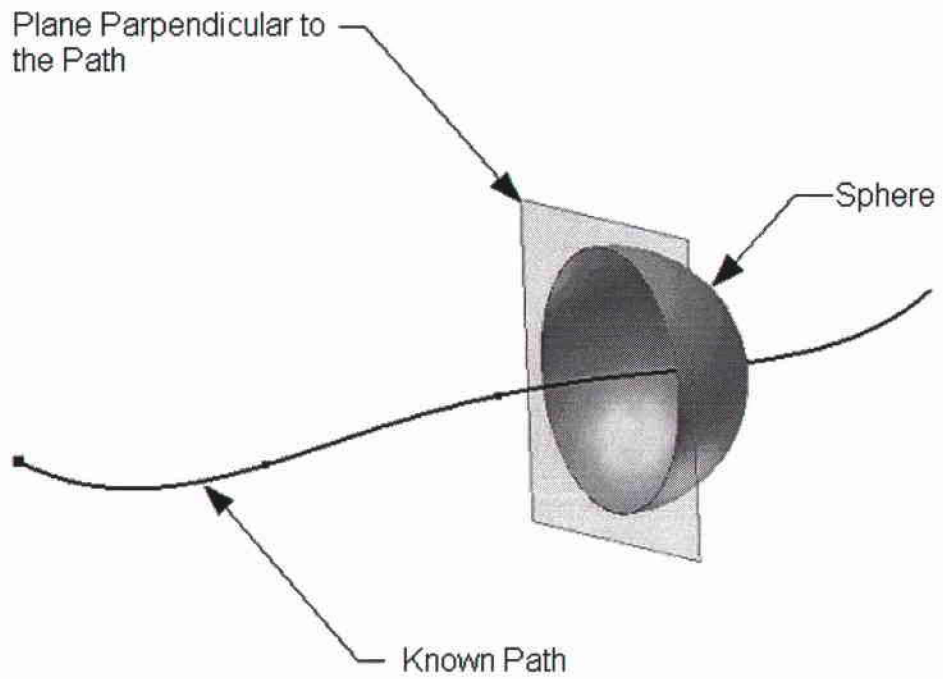


Figure 2-4 Resultant circles from the intersection between the sphere and the plane

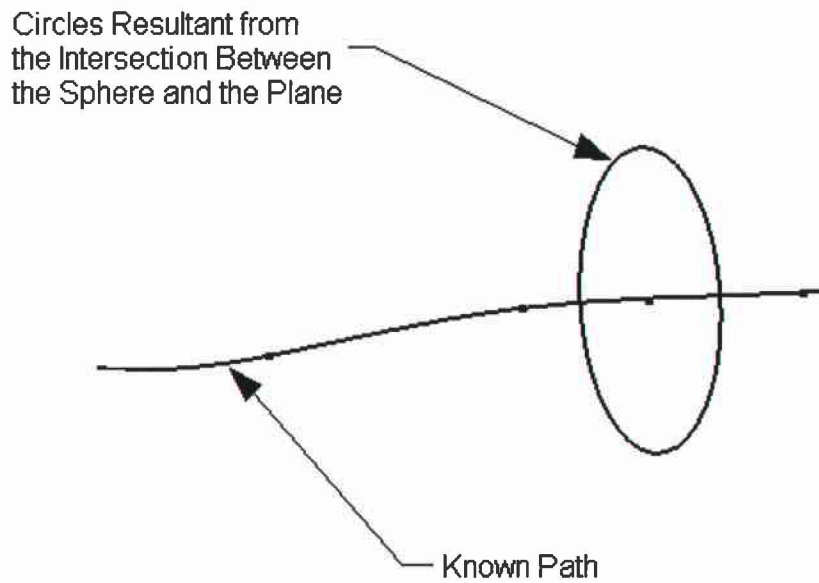


Figure 2-5 Circles perpendicular to the path

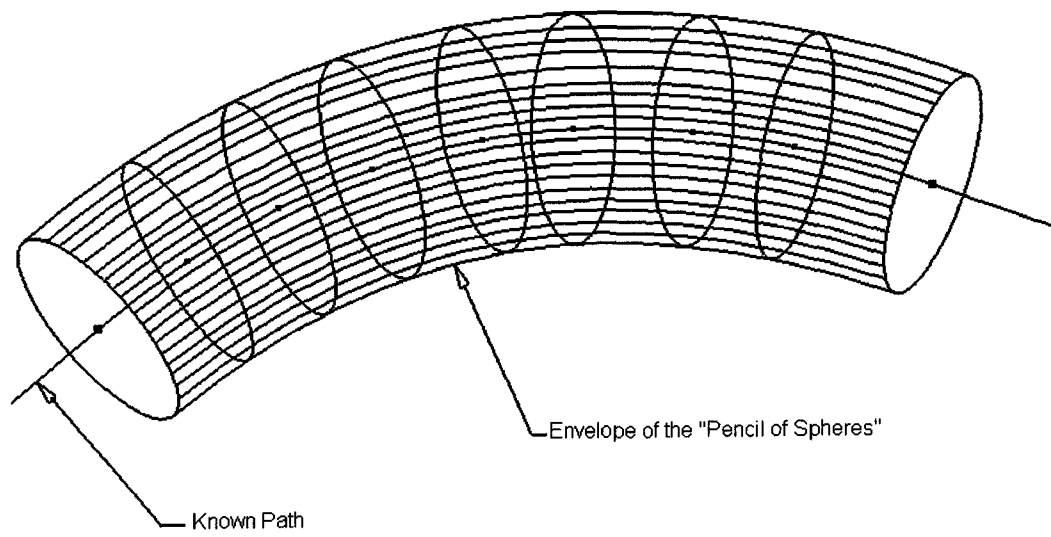


Figure 2-6 Envelope of the "Pencil of the Spheres"

CHAPTER 3

APPLICATION TO SINGLE HELICAL WIRE RODS

The model described in this chapter can be used for both right-hand-lay and left-hand-lay helical curves. The shape is only one in both cases.

3.1 Description of the Model

Using the approach described in Chapter 2, it is possible to determine the true shape of the helical round rods in the transverse cross-section of the rope. The steps necessary to develop this geometry are listed below.

1. Determine a parametric equation that describes the coordinates along a helical path. The parameter to be varied is the rotation angle, θ , defined in Figure 3.1.
2. Develop the Pencil of Spheres equation to create infinite spheres lying on this know helical path.
3. Take the derivative of Pencil of Spheres equation with respect to the rotation angle, θ . The resulting equation are planes perpendicular to the path that cut the spheres through their centers.
4. The simultaneous solution of these two equations yield the envelope of spheres moving along the helical curved path.
5. Intersect the “Pencil of Spheres” envelope with a plane perpendicular to the rope axis. This intersection represents the real cross-section of the helical wire rope.

3.2 Helical Centerline and Pencil of Spheres

The coordinates of the helical centerline laying on a circle of radius, R_p , and with a helical angle, α , are described by the following equations:

$$x_0 = R_p \cos \theta \quad (3.1)$$

$$y_0 = R_p \sin \theta \quad (3.2)$$

$$z_0 = \theta R_p \cot \alpha \quad (3.3)$$

In Figure 3.1 there is a graphic representation of this centerline. The global coordinate system is located with the “z” axis in the same position of the cable axis, and as a result the x-y plane is parallel to the cross-section of the cable. The difference between the coordinates of one point to another is in the parameter represented by the angle, θ . Applying the Pencil of Spheres to this centerline, the following equation is obtained:

$$\begin{aligned} (x - x_0)^2 + (y - y_0)^2 + (z - z_0)^2 &= R_w^2 \\ (x - R_p \cos \theta)^2 + (y - R_p \sin \theta)^2 + (z - \theta R_p \cot \alpha)^2 &= R_w^2 \end{aligned} \quad (3.4)$$

Equation 3.4 represents a sphere with radius, R_w , with its center lying on the position represented by the point (x_0, y_0, z_0) .

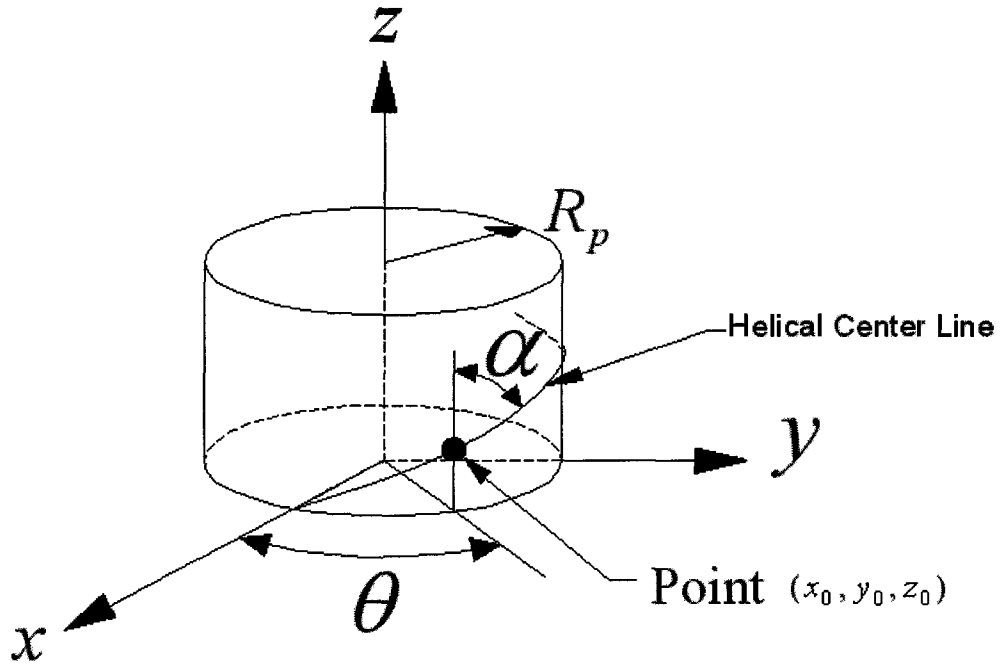


Figure 3-1 Coordinates of the centerline helical path

3.3 Application of Theory of Envelopes

Taking the derivative of Equation 3.4, and making this derivative equal to zero with respect to θ , leads to the following equations:

$$\frac{d}{d\theta}(\text{Equation } 3.4) = 0$$

$$2(x - R_p \cos \theta)(R_p \sin \theta) + 2(y - R_p \sin \theta)(-R_p \cos \theta) + 2(z - \theta R_p \cot \alpha)(-R_p \cot \alpha) = 0$$

$$x \sin \theta - y \cos \theta = \cot \alpha (z - \theta R_p \cot \alpha) \quad (3.5)$$

Equation (3.5) represents a plane perpendicular to the path and cuts the sphere in the middle. Solving equations (3.4) and (3.5) simultaneously, a circle with the same diameter

of the sphere is obtained. These circles are perpendicular to the path with their centers lying on the helical path. If an infinite number of circles are placed along the centerline of varying θ , the envelope describes the circular wire rod.

Intersecting every circle with some plane parallel to plane x-y produces two points. By solving for the range of θ where there are intersections with the mentioned plane, it yields the cross-section of the circular rod. For simplicity, the plane $z = 0$, is used.

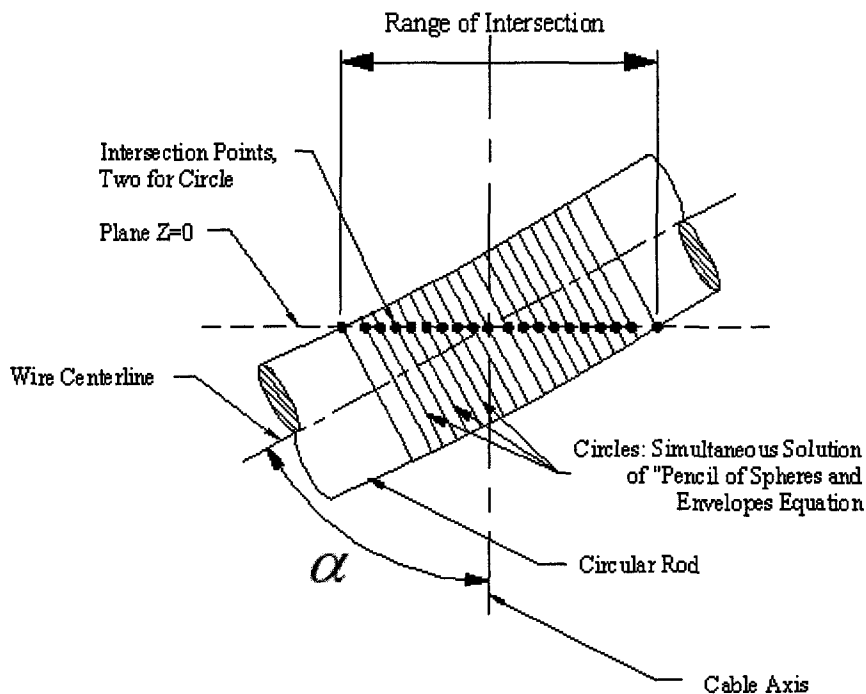


Figure 3-2 Intersection between circles and plane $z=0$

Figure 3.2 represents a piece of a circular wire rod lying on the helical path. In this figure it can be seen the range of intersection between the different circles and the plane $z = 0$. Every circle, resulting from the intersection of the Pencil of Spheres

equation and its derivative with respect to θ , equal to zero, intersect the plane, $z = 0$, at two points. This is represented in Figure 3.3.

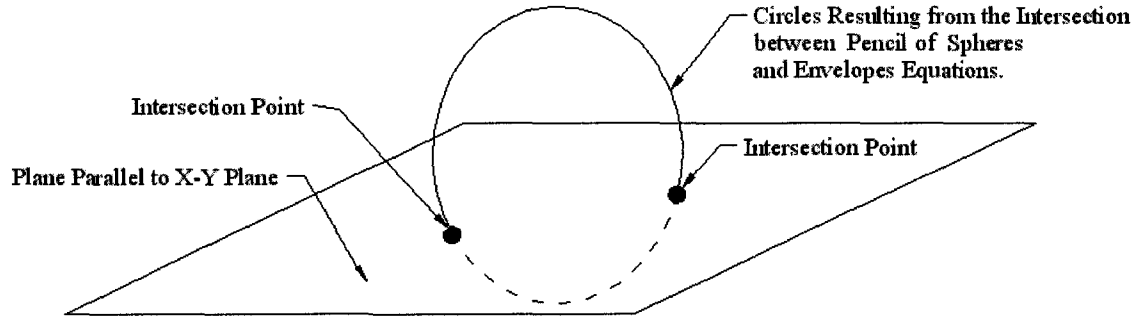


Figure 3-3 Intersection between one circle and some plane parallel to the cable cross-section

3.4 Intersection Between Circles and Plane $z=0$

As established before, the circles are obtained with the intersection between the Pencil of Spheres equation and its derivatives with respect to the parameter, θ , equal to zero. Solving simultaneously equations 3.4 and 3.5 and intersecting this result with plane $z = 0$, two points representing the intersection between the circle and plane $z = 0$ are obtained. The following equations represent this mathematically.

Equation 3.4:

$$(x - R_p \cos \theta)^2 + (y - R_p \sin \theta)^2 + (0 - \theta R_p \cot \alpha)^2 = R_w^2$$

$$x^2 + y^2 - 2xR_p \cos \theta - 2yR_p \sin \theta + R_p^2(1 + \theta^2 \cot^2 \alpha) - R_s^2 = 0 \quad (3.4a)$$

Equation 3.5:

$$x \sin \theta - y \cos \theta = \cot \alpha (0 - \theta R_p \cot \alpha)$$

$$x \sin \theta - y \cos \theta = -\theta R_p \cot^2 \alpha \quad (3.5a)$$

Two equations simultaneously:

$$x^2 + y^2 - 2xR_p \cos \theta - 2yR_p \sin \theta + R_p^2(1 + \theta^2 \cot^2 \alpha) - R_s^2 = 0$$

$$x \sin \theta - y \cos \theta = -\theta R_p \cot^2 \alpha$$

Substituting $g_1 = 2R_p \cos \theta$, $g_2 = 2R_p \sin \theta$, $g_3 = R_p^2(1 + \theta^2 \cot^2 \alpha) - R_s^2$, equation (3.4a)

can be written as follows:

$$x^2 + y^2 - g_1 x - g_2 y + g_3 = 0 \quad (3.4b)$$

From equation (3.5a), $y = \frac{\theta R_p \cot^2 \alpha}{\cos \theta} + x \tan \theta$, with $g_4 = \frac{\theta R_p \cot^2 \alpha}{\cos \theta}$ equation (3.5a)

can be written as

$$y = g_4 + x \tan \theta \quad (3.5b)$$

The two points resulting from the intersection between the circle and the plane $z = 0$ are obtained with the simultaneous solution of equations 3.4b and 3.5b. Combining these two equations produces a quadratic equation which solution gives these two points.

$$x^2(1 + \tan^2 \theta) + x(2g_4 \tan \theta - g_1 - g_2 \tan \theta) + g_4^2 - g_2 g_4 + g_3 = 0 \quad (3.6)$$

In fact equation (3.6) is a quadratic equation of the following type: $Ax^2 + Bx + c = 0$ and this equation has two solutions for the x variable.

3.5 Relationship Between the Covering Angle and the Helix Angle

The Figure 3-4 shows the geometric transformation for helical wire rods. The covering angle, θ , is determined by the following parameters:

- The pitch radius, R
- The wires radius, R_w
- The helix angle, α
- The number of wires, N_w

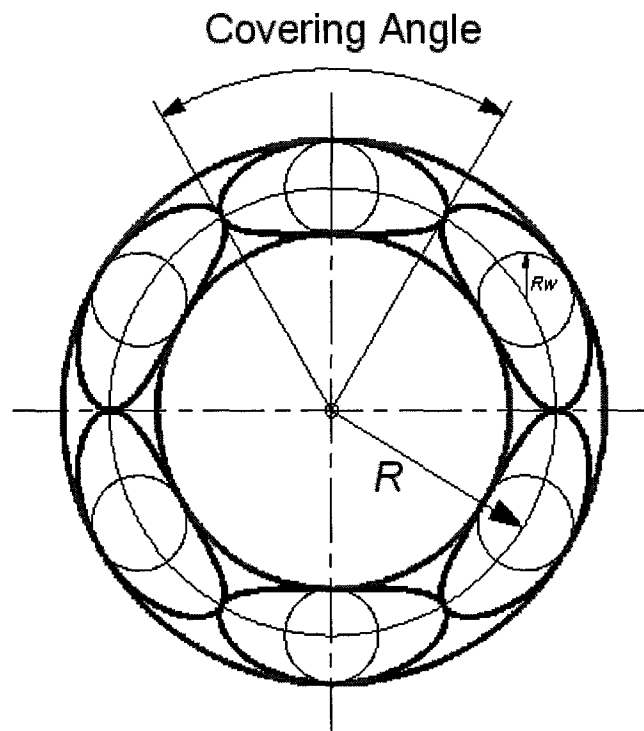


Figure 3-4 Cross-section of the helical wire rod

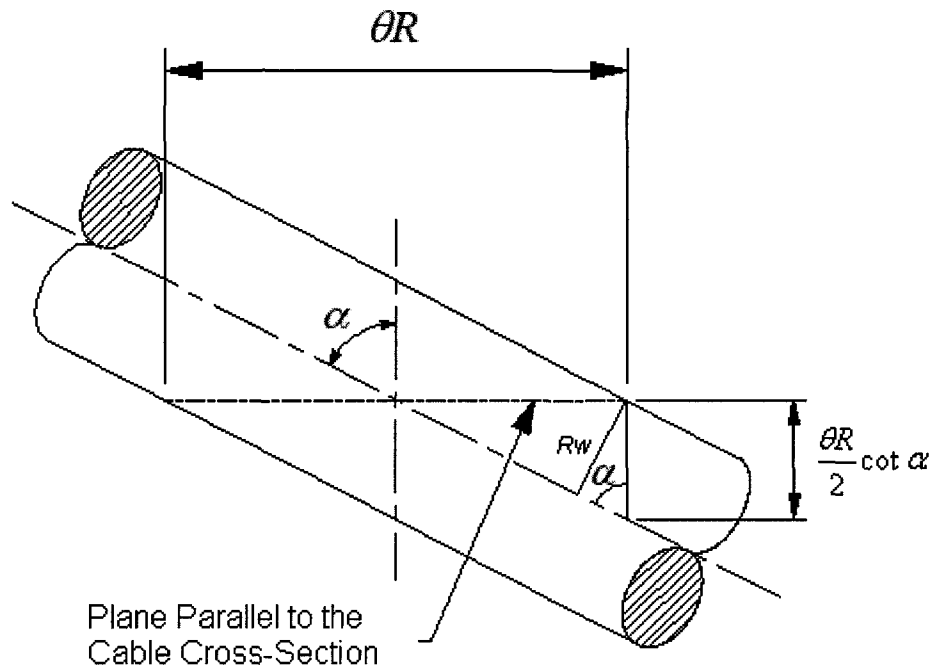


Figure 3-5 Piece of helical wire rod shows the relationship between the covering angle, θ , and the helix angle, α

Figure 3-5 shows the relationship between the covering angle, θ , and the maximum helix angle, α .

$$\frac{\theta R}{2} \cot \alpha \sin \alpha = R_w$$

$$\frac{\theta R}{2 R_w} = \frac{\tan \alpha}{\sin \alpha}$$

$$\theta = \frac{2 \pi}{N_w}$$

$$\frac{\pi R}{N_w R_w} = \frac{\tan \alpha}{\sin \alpha}$$

4.1 Final Representation of the Helical Wire Rod Cross-Section

Solving equation 3.6 simultaneously produces the cross-section. For the solution of Equation 3.6, the covering angle determined in Section 3.5 is used. Alternatively, it considers only the real values in the solution of the quadratic Equation 3.6. Using the approach described here and solving these equations for every angle, θ , where there is intersection with plane, $z = 0$, the final cross-section of the helical wire rod is obtained.

Figure 3.4 shows the final representation of the cross-section for a helical wire rod with the following characteristics:

- Diameter of the central core= 15 mm
- Diameter of the wires, $R_w = 4$ mm
- Number of wires, $N_w = 6$

The final numerical solution representation of this transformation produces a bean shape (fig. 3.4). The bean is more elongated if the helix angle increases and more circular if the angle decreases. If the helix angle is equal to zero, the shape is circular.

CHAPTER 4

APPLICATION TO DOUBLE HELICAL ROUND WIRES

This chapter shows the mathematical model that describes the cross-section of double helical wire rods. The model can be used for both, same and opposite lay directions of the first and second helix, but since there is a relationship between the first and second rotational angles, θ and ϕ , described in the next chapter, some arrangements have to be made for the equations used when the first and second helix are opposite to each other in direction. This arrangement is explained in Section 4.6. Figure 4.1 shows the laying directions and the convention sign used in this model.

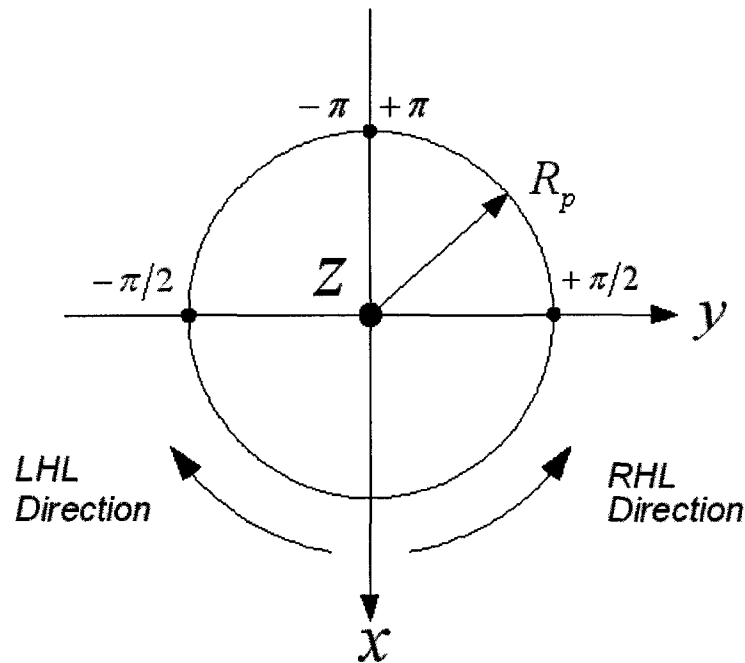


Figure 4-1 Convention sign used in the model

4.1 Three-Dimensional Coordinate System for Double Helix

Coordinate systems indicated in Figure 4.1 are used. The global z -axis is collinear with the cable axis, and the resulting global x - y plane is parallel to the transverse cross-section of the cable. A local coordinate system (x_s, y_s, z_s) is placed with the z -axis tangent to the helical path of the first helix centerline. This local coordinate system is moving when the rotational angle, θ , increases or decreases. Also when the rotational angle, θ , is zero both x -axis, local and global are collinear, this situation is shown in Figure 4.2. The first helix also lies on a circle with radius R_p . Using equations described for the single helix analysis, it is possible to know the coordinates of this centerline for every value of θ . Equations 3.1, 3.2 and 3.3 describe these coordinates. With this approach, it is possible to know the origin of the local coordinate system at every value of θ . The origin of the local coordinate system (x_s, y_s, z_s) has different positions depending on the rotational angle, θ , the radius R_p , and the helix angle, α .

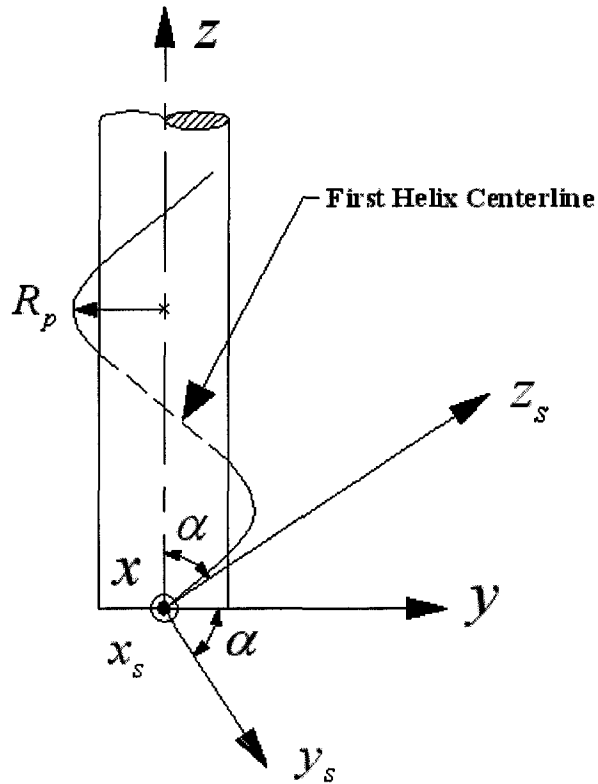


Figure 4-2 Coordinate system for double helical wire rods

Figure 4.3 shows a top view of the second helical wire rod. It can be seen that the global z -axis is collinear with the cable axis, and at the initial position, the global and local x -axes are also collinear. The pitch radius, R_{ss} , also is shown. The local z -axis is always tangent to the first helix centerline. The global x - y plane lies on the cable transverse cross-section. The local x - y plane forms an angle equal to α with respect to the cable transverse cross-section.

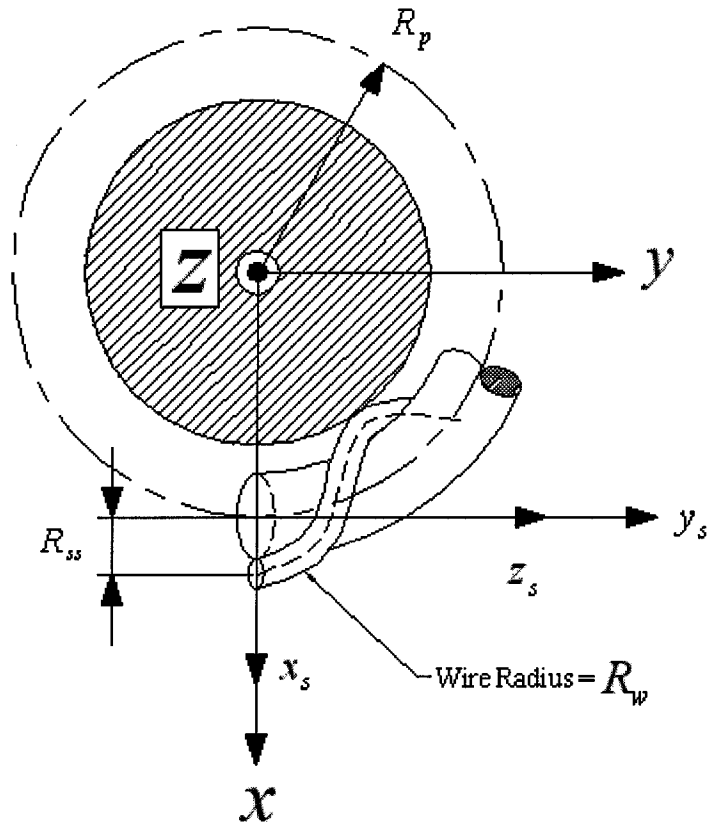


Figure 4-3 Top view of the second helical wire rod

4.2 Second Helix Centerline and Transformation to a Global Coordinate System

The second helix centerline lays around the first helix. Figure 4.4 shows how the coordinate of the second helix vary in the local coordinate system (x_s, y_s, z_s) . Plane x_s, y_s remains perpendicular to the first helical path as shown in Figure 4.4 (right side of Figure 4.4).

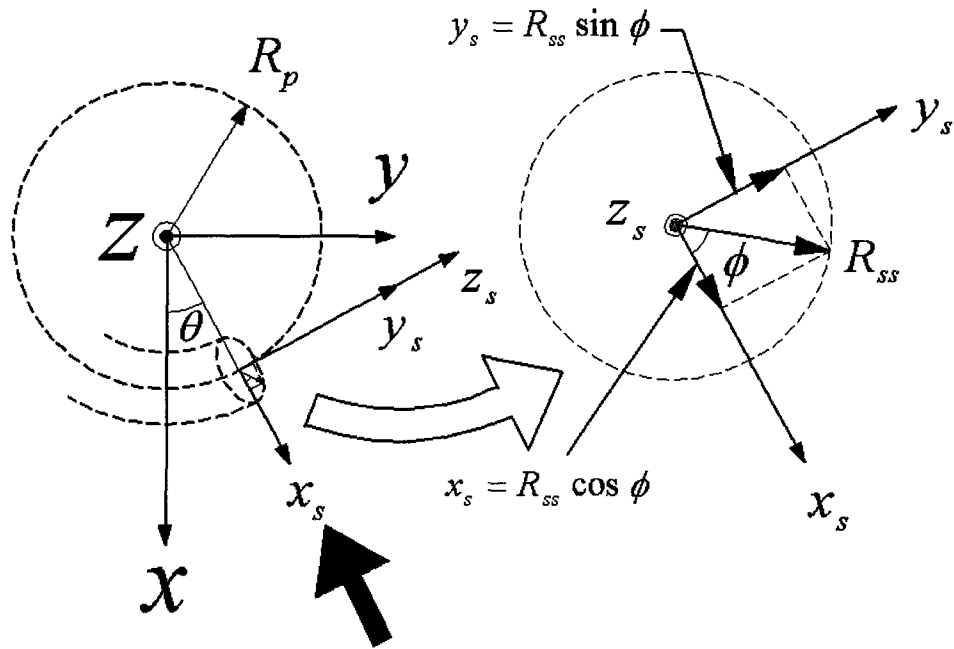


Figure 4-4 Coordinates of the second helix in the local coordinate system represented by the axes x_s, y_s

These coordinates are a function of radius, R_{ss} , and some parameter ϕ . The parameter ϕ represents the rotational angle of the second helix around the first helix. The x and y coordinates over this local coordinate system are represented in Figure 4.4, right side. The value corresponding to the z coordinate in this local system is always zero because this local coordinate system is moving along the helical path and the x_s, y_s plane always is perpendicular to the helical path. If this local coordinate system is rotated around the x_s -axis a certain amount, α , the global and local z -axes will remain parallel. As a result, global and local planes x - y will remain parallel too. A view from the direction of the black arrow indicated in Figure 4.4, shows this first coordinate transformation around the x_s -axis. Figure 4.5 shows this coordinated transformation. It can be seen that the z -axis, local and global axes remain parallel after this transformation as the x - y global and local

planes do also. This new coordinate system is represented by the coordinate frame,

$$x'_s, y'_s, z'_s$$

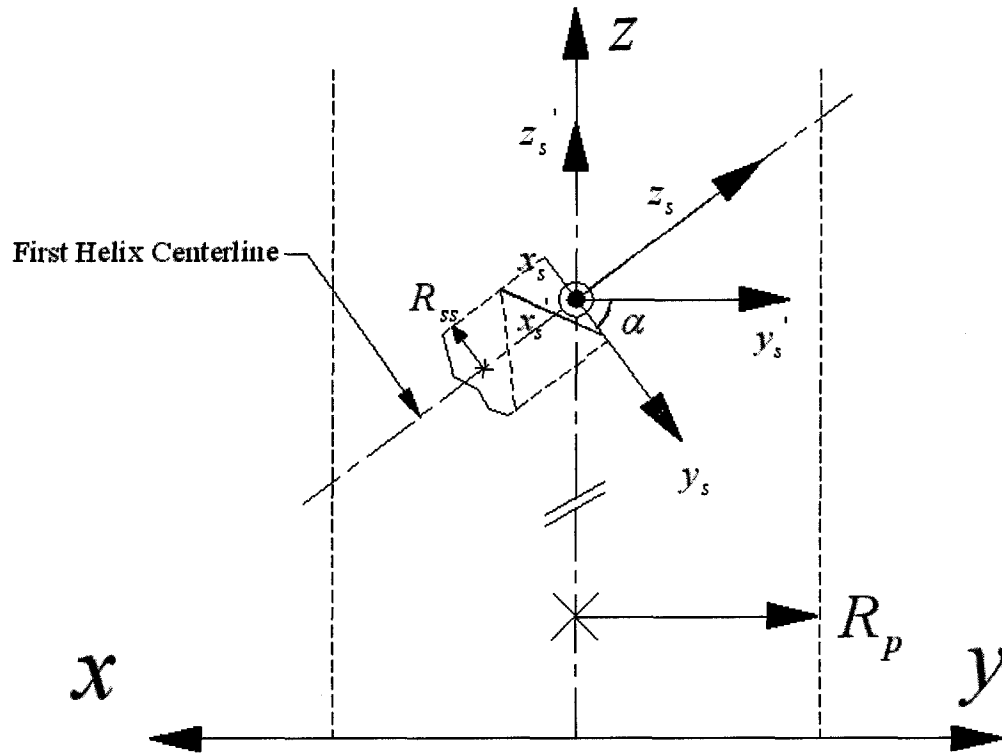


Figure 4-5 First coordinate transformation

This coordinate transformation can be expressed mathematically by the following set of equations:

$$\begin{Bmatrix} y'_s \\ z'_s \\ x'_s \end{Bmatrix} = \begin{bmatrix} \cos \alpha & \sin \alpha & 0 \\ -\sin \alpha & \cos \alpha & 0 \\ 0 & 0 & 1 \end{bmatrix} \begin{Bmatrix} y_s \\ z_s = 0 \\ x_s \end{Bmatrix} \quad (4.1)$$

$$y'_s = y_s \cos \alpha = R_{ss} \cos \alpha \sin \phi \quad (4.2)$$

$$z'_s = -y_s \sin \alpha = -R_{ss} \sin \alpha \sin \phi \quad (4.3)$$

$$x'_s = x_s \quad (4.4)$$

the coordinates x'_s and x_s are collinear (Figure 4.3) and $x_s = R_{ss} \cos \phi$. Now the coordinates of the second helical centerline is known in this new local coordinate system. Figure 4.6 shows another rotation around the z'_s -axis, where the angle of rotation is equal to the angle, θ . This new coordinate system is represented by the coordinate system x', y', z' . In this new coordinate system the three axes are parallel to the axes in the global coordinate system.

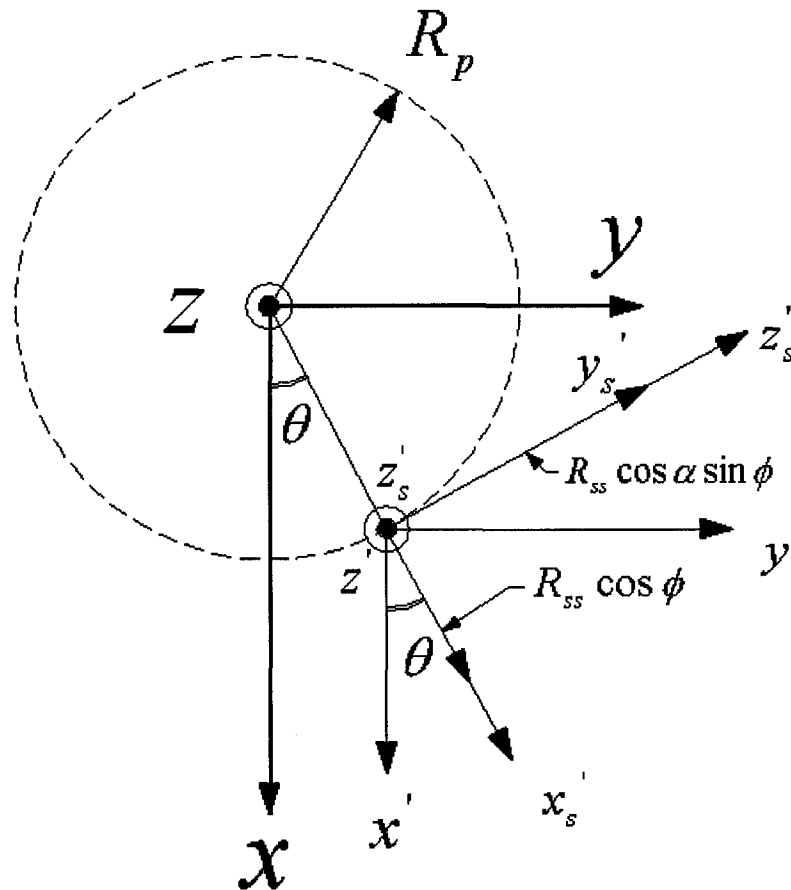


Figure 4-6 Second coordinate transformation about z'_s axis

This coordinate transformation is described by the following equations:

$$\begin{Bmatrix} x'_s \\ y'_s \\ z'_s \end{Bmatrix} = \begin{bmatrix} \cos \theta & \sin \theta & 0 \\ -\sin \theta & \cos \theta & 0 \\ 0 & 0 & 1 \end{bmatrix} \begin{Bmatrix} x' \\ y' \\ z' \end{Bmatrix} \quad (4.5)$$

$$\begin{Bmatrix} x' \\ y' \\ z' \end{Bmatrix} = \begin{bmatrix} \cos \theta & \sin \theta & 0 \\ -\sin \theta & \cos \theta & 0 \\ 0 & 0 & 1 \end{bmatrix}^{-1} \begin{Bmatrix} x'_s \\ y'_s \\ z'_s \end{Bmatrix} = \begin{bmatrix} \cos \theta & -\sin \theta & 0 \\ \sin \theta & \cos \theta & 0 \\ 0 & 0 & 1 \end{bmatrix} \begin{Bmatrix} x'_s \\ y'_s \\ z'_s \end{Bmatrix} \quad (4.6)$$

$$\begin{Bmatrix} x' \\ y' \\ z' \end{Bmatrix} = \begin{bmatrix} \cos \theta & -\sin \theta & 0 \\ \sin \theta & \cos \theta & 0 \\ 0 & 0 & 1 \end{bmatrix} \begin{Bmatrix} x'_s \\ y'_s \\ z'_s \end{Bmatrix} \quad (4.6a)$$

$$x' = x'_s \cos \theta - y'_s \sin \theta \quad (4.7)$$

$$y' = x'_s \sin \theta + y'_s \cos \theta \quad (4.8)$$

$$z' = z'_s \quad (4.9)$$

Finally, replacing values the following coordinates in this new local coordinate system

(x', y', z') become

$$x' = R_{ss} \cos \theta \cos \phi - R_{ss} \sin \theta \sin \phi \cos \alpha \quad (4.10)$$

$$y' = R_{ss} \sin \theta \cos \phi + R_{ss} \cos \theta \sin \phi \cos \alpha \quad (4.11)$$

$$z' = -R_{ss} \sin \phi \sin \alpha \quad (4.12)$$

4.3 Coordinates of the Second Helix in the Global Coordinate System x - y - z

Knowing the coordinates of the first helix, and that the origin of this new coordinate system lies on this helical path (equation 3.1, 3.2 and 3.3), it is possible to obtain the coordinates of the second helix in this global coordinate system according to

$$x_{dh} = R_p \cos \theta + x'$$

$$y_{dh} = R_p \sin \theta + y'$$

$$z_{dh} = \theta R_p \cot \alpha + z'$$

$$x_{dh} = R_p \cos \theta + R_{ss} (\cos \theta \cos \phi - \sin \theta \sin \phi \cos \alpha) = f_1$$

$$y_{dh} = R_p \sin \theta + R_{ss} (\sin \theta \cos \phi + \cos \theta \sin \phi \cos \alpha) = f_2$$

$$z_{dh} = \theta R_p \cot \alpha - R_{ss} \sin \phi \sin \alpha = f_3$$

The subscript dh (double helix) means coordinates of the points over the second helix in the global x - y - z coordinate system. For simplification, the last three equations that represent the second helix centerline are called f_1 , f_2 and f_3 .

4.4 Application of Pencil of Spheres Equation and Theory of Envelopes to Double Helix Centerline

Because the centerline of the second helix is known, it is possible to place spheres along this centerline using the equation pencil of spheres. This mathematical operation is represented by the following equation:

$$(x - f_1)^2 + (y - f_2)^2 + (z - f_3)^2 - R_w^2 = 0 = F \quad (4.19)$$

Equation 4.19 represents a sphere with radius, R_w , laying on the second helix centerline, specifically at the point represented by the coordinates f_1, f_2 and f_3 . Applying the theory of envelopes to this equation (the derivative of this equation with respect to the parameters θ and ϕ), and making this equation equal to zero, a plane perpendicular to the second helix centerline that cuts the sphere through its center is obtained. This is represented in Figure 2.3 and 2.4. The resultant equations for this derivative are the following:

$$\frac{\partial F}{\partial \theta} + \frac{\partial F}{\partial \phi} = 0 \quad (4.20)$$

$$\frac{\partial F}{\partial \theta} = 2(x - f_1) \left(\frac{-\partial f_1}{\partial \theta} \right) + 2(y - f_2) \left(\frac{-\partial f_2}{\partial \theta} \right) + 2(z - f_3) \left(\frac{-\partial f_3}{\partial \theta} \right)$$

$$\frac{\partial F}{\partial \phi} = 2(x - f_1) \left(\frac{-\partial f_1}{\partial \phi} \right) + 2(y - f_2) \left(\frac{-\partial f_2}{\partial \phi} \right) + 2(z - f_3) \left(\frac{-\partial f_3}{\partial \phi} \right)$$

$$\frac{\partial f_1}{\partial \theta} = f_4 \quad (4.21)$$

$$f_4 = -R_p \sin \theta + R_{ss} (-\sin \theta \cos \phi - \cos \theta \sin \phi \cos \alpha) \quad (4.21a)$$

$$\frac{\partial f_2}{\partial \theta} = f_5 \quad (4.22)$$

$$f_5 = R_p \cos \theta + R_{ss} (\cos \theta \cos \phi - \sin \theta \sin \phi \cos \alpha) \quad (4.22a)$$

$$\frac{\partial f_3}{\partial \theta} = f_6 \quad (4.23)$$

$$f_6 = R_p \cot \alpha \quad (4.23a)$$

$$\frac{\partial f_1}{\partial \phi} = f_7 \quad (4.24)$$

$$f_7 = R_{ss} (-\cos \theta \sin \phi - \sin \theta \cos \phi \cos \alpha) \quad (4.24a)$$

$$\frac{\partial f_2}{\partial \phi} = f_8 \quad (4.25)$$

$$f_8 = R_{ss} (-\sin \theta \sin \phi + \cos \theta \cos \phi \cos \alpha) \quad (4.25a)$$

$$\frac{\partial f_3}{\partial \phi} = f_9 \quad (4.26)$$

$$f_9 = -R_{ss} \cos \phi \sin \alpha \quad (4.26a)$$

Equation 4.20 is transformed by the following linear equation:

$$(x - f_1)(-f_4 - f_7) + (y - f_2)(-f_5 - f_8) + (z - f_3)(-f_6 - f_9) = 0 \quad (4.27)$$

Now with

$$(-f_4 - f_7) = f_{10} \quad (4.28)$$

$$(-f_5 - f_8) = f_{11} \quad (4.29)$$

$$(-f_6 - f_9) = f_{12} \quad (4.30)$$

Equation 4.27 takes the following form:

$$(x - f_1)f_{10} + (y - f_2)f_{11} + (z - f_3)f_{12} = 0 \quad (4.31)$$

The intersections between equation 4.19 and 4.31 represent circles with their centers laying on the second helix centerline, and also these circles are perpendicular to the helical path. The same was shown in Figure 2.5.

4.5 Intersecting the Circles with a Plane Parallel to Plane x-y

Using the Theory of Envelopes and the equation of the Pencil of Spheres, it is possible to obtain circles with a radius equal to the helical wire rod, with their centers laying on a second helical path. These circles are represented by the intersection or simultaneous solution of Equations 4.19 and 4.31. If these circles are intersected with a plane parallel to the cross-section of the cable, the final shape of this wire in such transverse plane is obtained. In this analysis, for simplicity, the plane $z=0$ with Equations 4.19 and 4.31 were transformed in the following equations:

$$(x - f_1)^2 + (y - f_2)^2 + (-f_3)^2 - R_w^2 = 0 \quad (4.32)$$

$$(x - f_1)f_{10} + (y - f_2)f_{11} - f_3f_{12} = 0 \quad (4.33)$$

Solving equation 4.33 for y in terms of x , the following solution is obtained:

$$y = \frac{f_3f_{12}}{f_{11}} + f_2 + \frac{f_1f_{10}}{f_{11}} - x \frac{f_{10}}{f_{11}} \quad (4.34)$$

Where

$$\frac{f_3f_{12}}{f_{11}} + f_2 + \frac{f_1f_{10}}{f_{11}} = f_{13} \quad (4.35)$$

$$-\frac{f_{10}}{f_{11}} = f_{14} \quad (4.36)$$

and the following linear equation:

$$y = f_{13} + xf_{14} \quad (4.37)$$

Placing values of Equation 4.37 into Equation 4.32, the following quadratic equation is found:

$$x^2(1 + f_{14}^2) + 2x(-f_1 + f_{13}f_{14} - f_2f_{14}) + f_1^2 + f_2^2 + f_3^2 + f_{13}^2 - 2f_2f_{13} - R_w^2 = 0 \quad (4.38)$$

Renaming the following terms,

$$(1 + f_{14}^2) = A \quad (4.39)$$

$$2(-f_1 + f_{13}f_{14} - f_2f_{14}) = B \quad (4.40)$$

$$f_1^2 + f_2^2 + f_3^2 + f_{13}^2 - 2f_2f_{13} - R_w^2 = C \quad (4.41)$$

Equation 4.38 can be written as the quadratic equation:

$$x^2A + xB + C = 0 \quad (4.42)$$

Equation 4.42 represents the intersection between a circle resulting from the intersection or simultaneous solution between the equation of the Pencil of Spheres and its derivative with respect to parameters θ and ϕ , equal to zero, and plane $z=0$. In fact, this represents the intersection between a circle with the same diameter of the wire rods with its center on the double helix centerline.

4.6 Mathematical Arrangement Used when Two Helix Have Opposite Direction

Figure 4.6 shows the case when two helix angles have opposite directions.

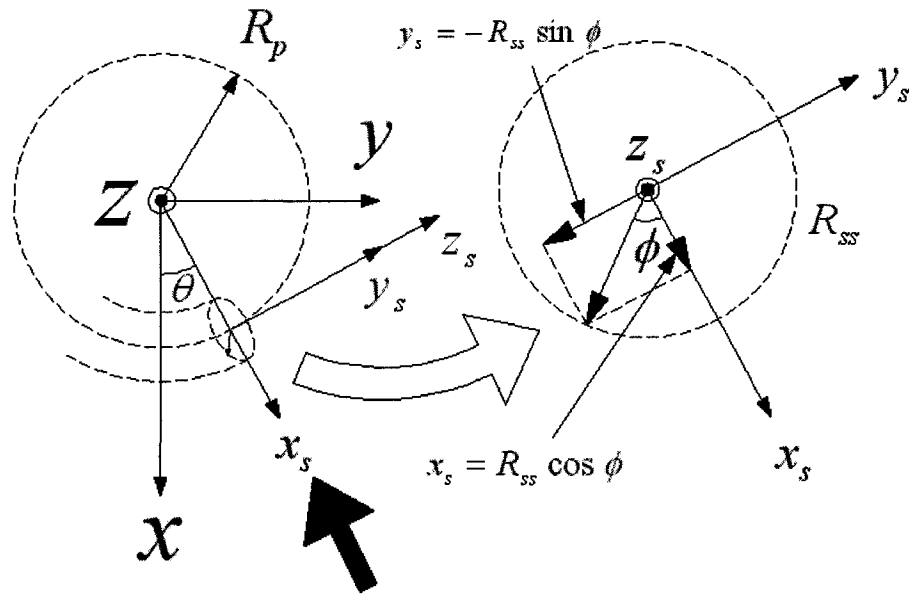


Figure 4-7 Coordinates of the second helix centerline when two helix angles are opposite in direction.

When the direction of the second helix is opposite to the first helix, the coordinates of the second helix centerline in the local coordinate system is represented by the following equations:

$$x_s = R_{ss} \cos \phi$$

$$y_s = -R_{ss} \sin \phi$$

Using the same approach as described in Section 4.2, the second helix centerline and transformation to a global coordinate system is obtained from the following equations for this case:

$$f_1 = R_p \cos \theta + R_{ss} (\cos \theta \cos \phi + \sin \theta \sin \phi \cos \alpha)$$

$$f_2 = R_p \sin \theta + R_{ss} (\sin \theta \cos \phi - \cos \theta \sin \phi \cos \alpha)$$

$$f_3 = \theta R_p \cot \alpha + R_{ss} \sin \phi \sin \alpha$$

$$f_4 = -R_p \sin \theta + R_{ss} (-\sin \theta \cos \phi + \cos \theta \sin \phi \cos \alpha)$$

$$f_5 = R_p \cos \theta + R_{ss} (-\cos \theta \cos \phi - \sin \theta \sin \phi \cos \alpha)$$

$$f_6 = R_p \cot \alpha$$

$$f_7 = R_{ss} (-\cos \theta \sin \phi + \sin \theta \cos \phi \cos \alpha)$$

$$f_8 = R_{ss} (-\sin \theta \sin \phi - \cos \theta \cos \phi \cos \alpha)$$

$$f_9 = R_{ss} \cos \phi \sin \alpha$$

The above equations represent the case when two helix angles have opposite direction. Placing these equations into the mathematical model the cross-section of the double helix with a different helix direction is obtained.

CHAPTER 5

NUMERICAL SOLUTION

5.1 Relationship Between First Rotational Angle, θ , and Second Rotational Angle, ϕ

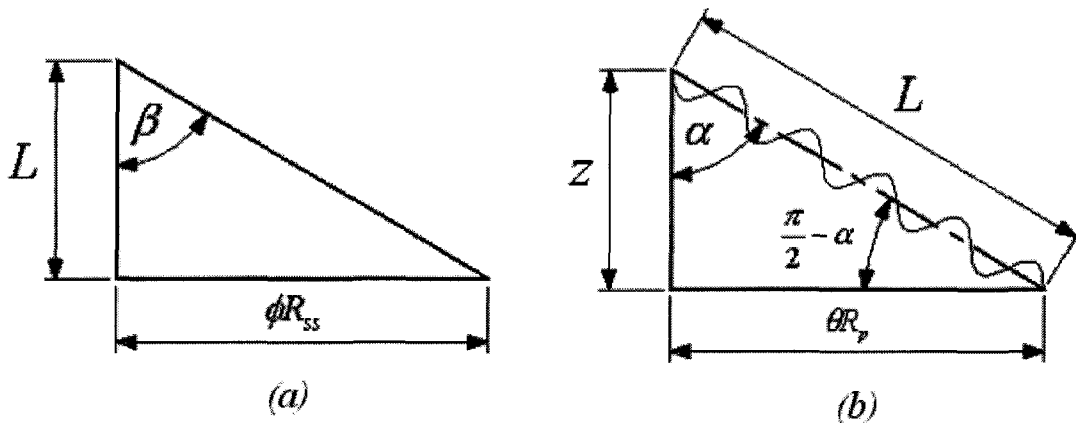


Figure 5-1 Relationship between θ and α

Figure 5.1(a) shows the developed geometry for the second helix, and Figure 5.1(b) shows the second helix over the first helix. The z value in the second helix corresponds to the L value of the first helix. With this relationship, it is possible to obtain one rotation angle as a function of the other. The mathematical relationship is described by the following equations:

From Figure 5.1(b) $L \cos\left(\frac{\pi}{2} - \alpha\right) = \theta R_p$ and from Figure 5.1(a) $L = \phi R_{ss} \cot \beta$.

Combining them, final relationship between ϕ and θ is given by:

$$\phi = \theta \frac{R_p \tan \beta}{R_{ss} \sin \alpha} \quad (5.1)$$

5.2 Numerical Analysis to Obtain the Resultant Transverse Cross-Section for Double Helical Wire Rods.

Because the strand has some known diameter as shown in Figure 5.2, it is possible to apply the procedure described in Section 3.4 and determine the covering angle for any strand, and as a result determine the maximum helix angle for the complete strand, α . Solving for every θ , from the different θ dependent equations from f_1 to f_{14} , it is possible to know their values and posteriori to solve Equation 4.42. Solving this equation for some θ , two x values will be known. Placing these two x values into Equation 4.37 will result in two y values. This represent two points that intersect plane $z=0$. When there is not an intersection between the circle and the plane $z=0$, the values of the square root solving Equation 4.42 has a negative value. The program that solves these simultaneous equations only consider values of θ where there are intersections given by $B^2 - 4AC \geq 0$.

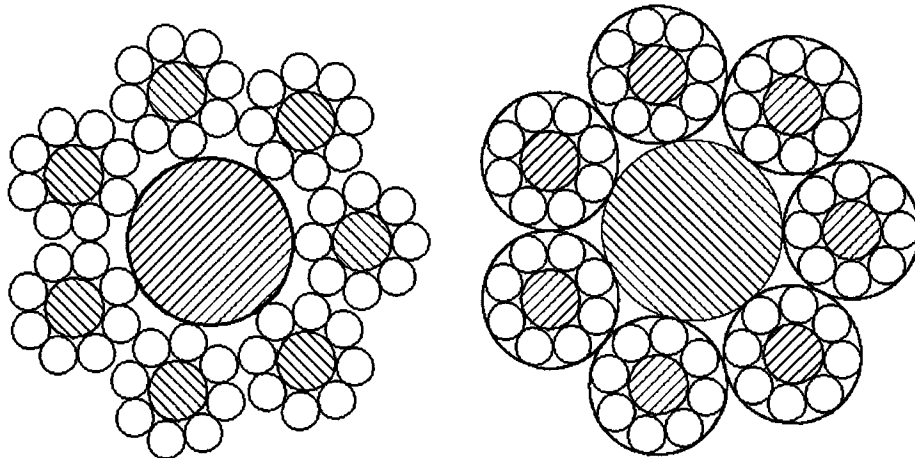


Figure 5-2 Double helical wire rod cable with seven strands

5.3 Considering More Than One Wire

As real strands are formed by more than one wire, the program has to determine for every wire its centerline. In Figure 5.3, a cross-section for double helical wire rods (schematic representation) are shown. This figure is only a schematic for both helical angles equal to zero that shows circular shapes, also in this figure is shown the nomenclature used in the model. To determine the centerline of every wire, the program considers x_s and y_s values according to the equations

$$x_s = R_{ss} \cos\left(\phi + \frac{2m\pi}{N_w}\right)$$

$$y_s = R_{ss} \sin\left(\phi + \frac{2m\pi}{N_w}\right)$$

The m parameter varies from 0 to $N_w - 1$, where N_w represents the number of wires in the strand. The z_s values do not change because these values are always zero, as explained in Section 4.2. In Figure 5.4, every black dot represents for every wire, its centerline in the plane $x_s - y_s$.

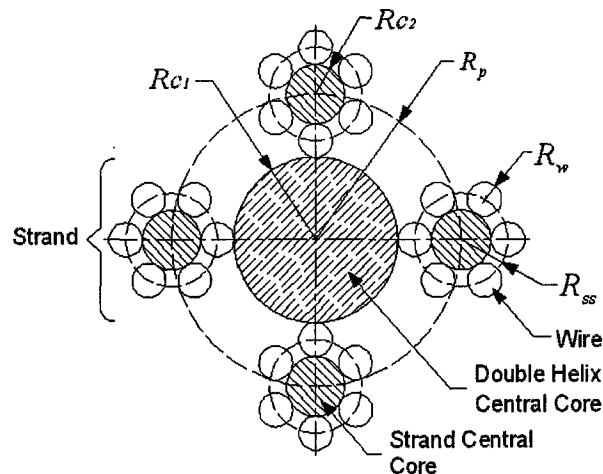


Figure 5-3 Nomenclature used in double helical wire rods

For example, for wire number 2 the real angle to consider is $\phi + \frac{2(1)\pi}{N_w}$ because for wire number two, m is equal to 1. With this approach the program determines every centerline and solves for the complete strand shape in the cross-section plane.

To draw all the strands in the double helical cross-section the program only needs to copy the points calculated in this step according to the number of strands in the wire rope.

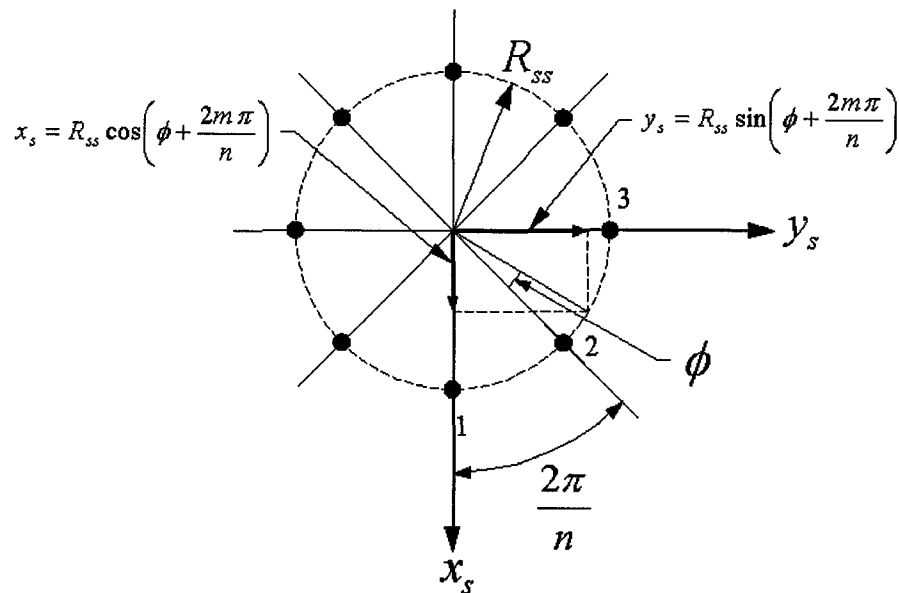


Figure 5-4 Considering more than one wire in the strand

5.4 Flow Chart for Numerical Analysis

Figure 5.5 shows the flow chart to solve for the cross-section of a double helical wire rods. The first box in the diagram requests input information related to the following parameters:

- Diameter of the wire rope central core

- Diameter of the strand central core
- Diameter of the wire
- Number of wires
- Number of strand
- Direction. If the second helix has same direction of the first helix this value is +1 and if the second helix has opposite direction than the first helix this value is -1

With the input information the program determines the two helix angles. For that purpose the program uses the approach described in Section 3.5 according to the following equations

$$\frac{\pi(R_{C2} + R_w)}{N_w R_w} = \frac{\tan \beta}{\sin \beta} \quad (5.2)$$

$$\frac{\pi(R_{C1} + 2R_w + R_{C2})}{N_s (R_{C2} + 2R_w)} = \frac{\tan \alpha}{\sin \alpha} \quad (5.3)$$

As the values in the left side of these equations are known, with iterations the two angles α and β can be found.

With the calculation of the two helix angles and all the parameters related to the elements used in the manufacture of the strand, the program determines the cross-section of these elements (strand elements). With the purpose that the program user watches and analyzes the strand transverse cross-section used in the design of the double helix wire rods, a model is displayed on the screen. When user clicks any key in the keyboard, the program continues with the calculations.

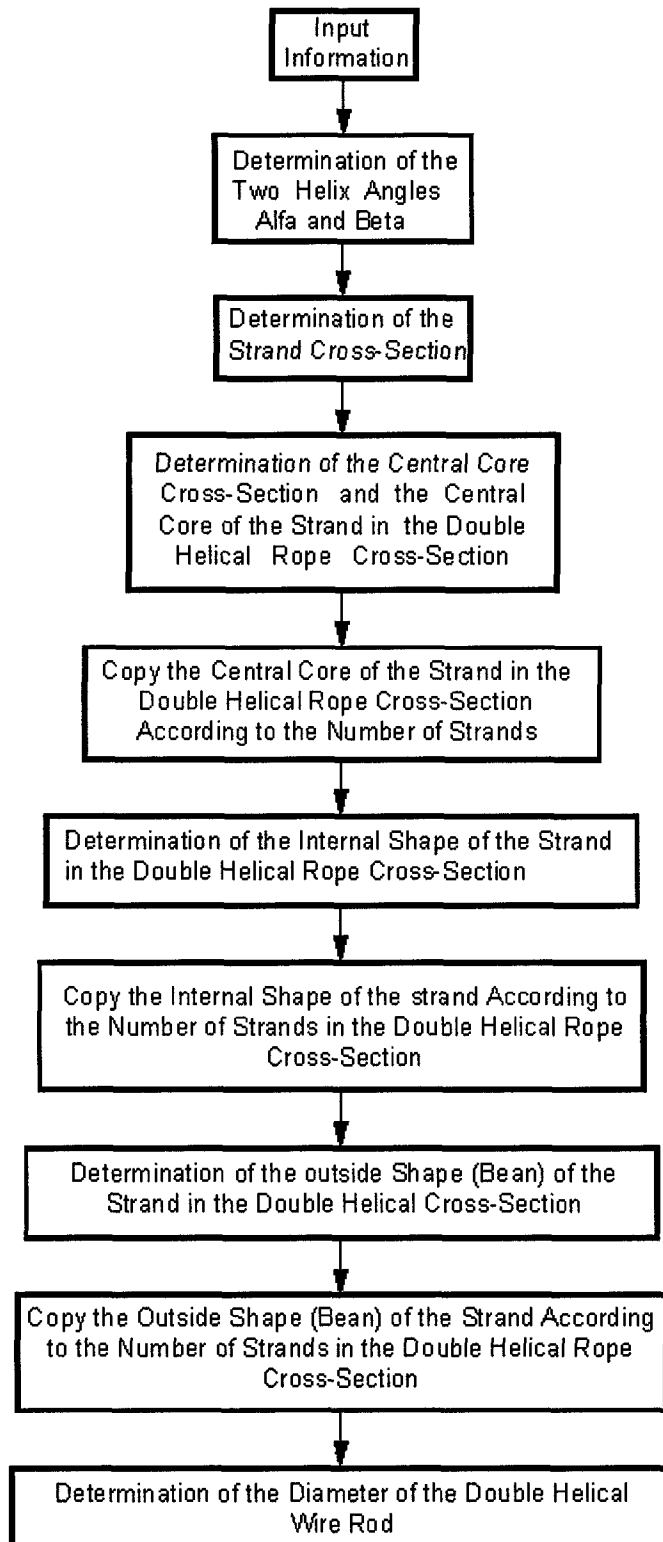


Figure 5-5 Flow chart for numerical solution

The next step in the program is to determine and draw the central circle corresponding to the central core of the double helical cross-section. Also at this point the program determines the points that correspond to the central core of the strand in the double helical cross-section. As shown in Figure 5.6, the inside bean represents this shape.

Using the approach described in Chapter 4, the program determines the internal shape of the double helical cross-section as shown in Figure 5.6. All these shapes (internal shape, inside bean and outside bean) are then copied according to the number of strands.

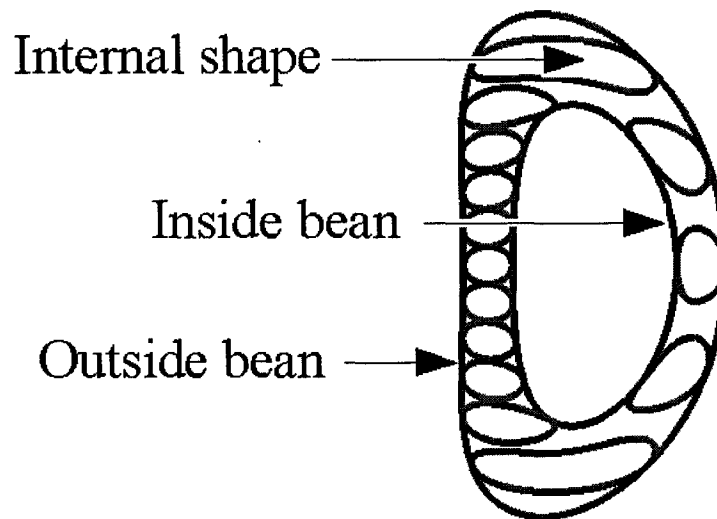


Figure 5-6 One complete strand in the double helical cross-section

CHAPTER 6

VERIFICATION OF THE MODEL

In this chapter, several examples that validate the mathematical model developed in this research are described. One example is the fact that the double helical shape for wires is drawn between the boundary of the outside bean and inside bean. Other important evidence is that the internal shape or double helix wires are drawn tangent to the outside and inside bean. The most important evidence is the verification and comparison with a real model. A real cable with high helix angles is not possible to find in the market, so a polyurethane model of a double helix was fabricated.

6.1 Internal Shapes of the Double Helix Wire Rods and the Contact Points with Outside Bean and Inside Bean

Figure 6.1 shows how all points of intersections between the beans and the internal shapes are tangent. Like in a real model, the wires only touch the central core at one point, and that means the two tangent curves, represented by black dots. In the same way, the wires touch the outside bean (imaginary) at only one point. The other important evidence is that gaps are produced in the outer diameter. This situation is similar to bending an extension spring. When this kind of spring is bent in the outer diameter, the wires that were touching each other are separated by this action, like in an extension spring, the inner diameter of wires are agglomerated around the central wire.

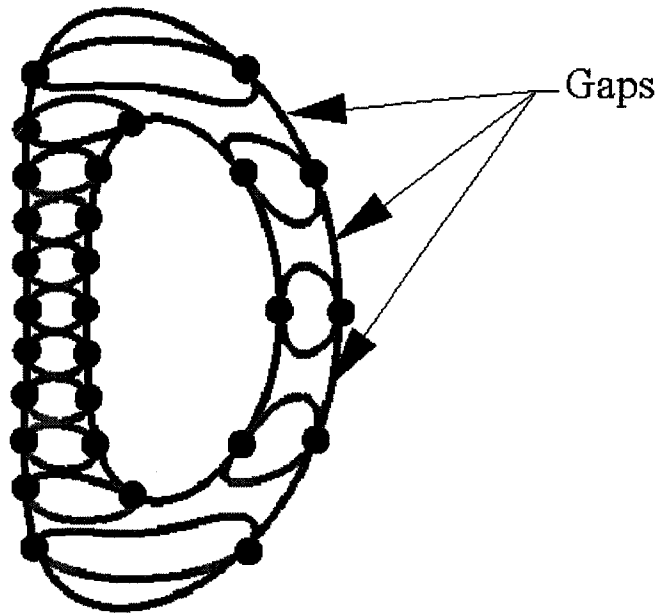


Figure 6-1 Points of intersection between outside bean, inside bean and internal shapes

6.2 Verification and Comparison with a Physical Model

Using the mathematical model described within this investigation, the algorithm first determines the cross-section of the strands used in the design of the double helical wire rods. This cross-section is known beforehand and can be drawn by some software available in the market. Figure 6-2 shows the transverse cross-section for the strand used in the physical model with the following specifications:

- Strand central core = 15 mm.
- Wire diameter = 4 mm.
- Number of wires = 6

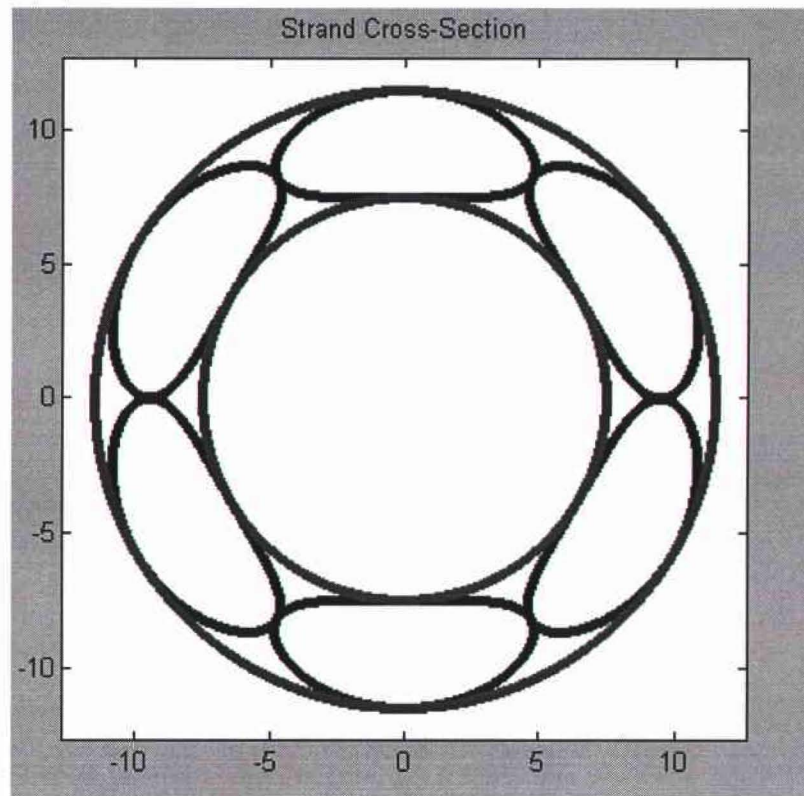


Figure 6-2 Strand cross-section

The following figures show the cross-section of a double helical wire rods with the following specifications:

- Double helical wire rod central core diameter = 50 mm.
- Strand central core diameter = 15 mm.
- Wire diameter = 4 mm
- Number of wires = 6
- Number of strands = 4

There are two possible models for the cross section of the double helical wire rod. One model corresponds to that when the two helix angles have the same direction, and the other model when the two helix angles have opposite direction. Figure 6-3 shows

the transverse cross-section of a double helical wire rod when the angles of the first and second helix have same directions, hence both are right-hand-lay or left-hand-lay.

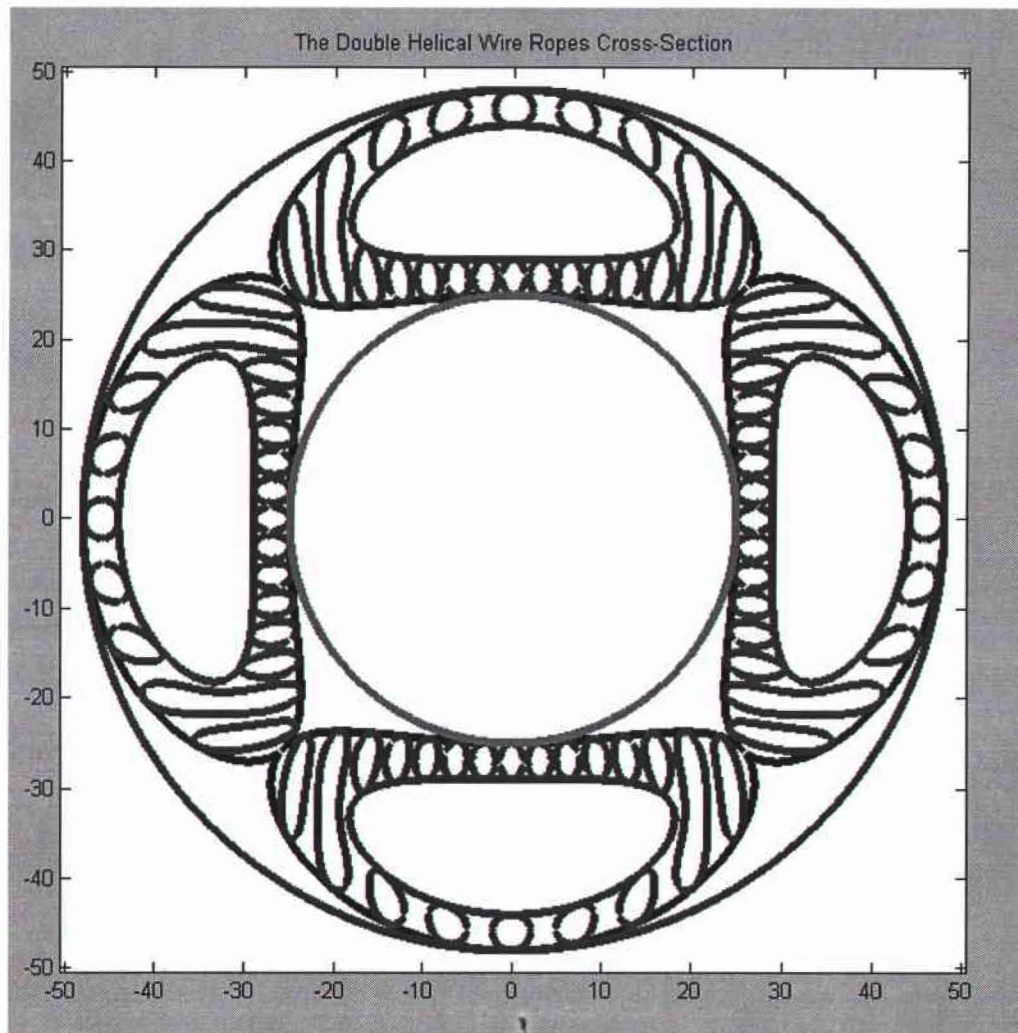


Figure 6-3 Double helical wire rod cross-section with two helix angles having same direction

Figure 6-4 shows the transverse cross-section of a double helical wire rods when the helix angles, first and second, have opposite directions, that is whichever of the following combinations:

- Right-hand-lay with Left-hand-lay

- Left-hand-lay with Right-hand-lay

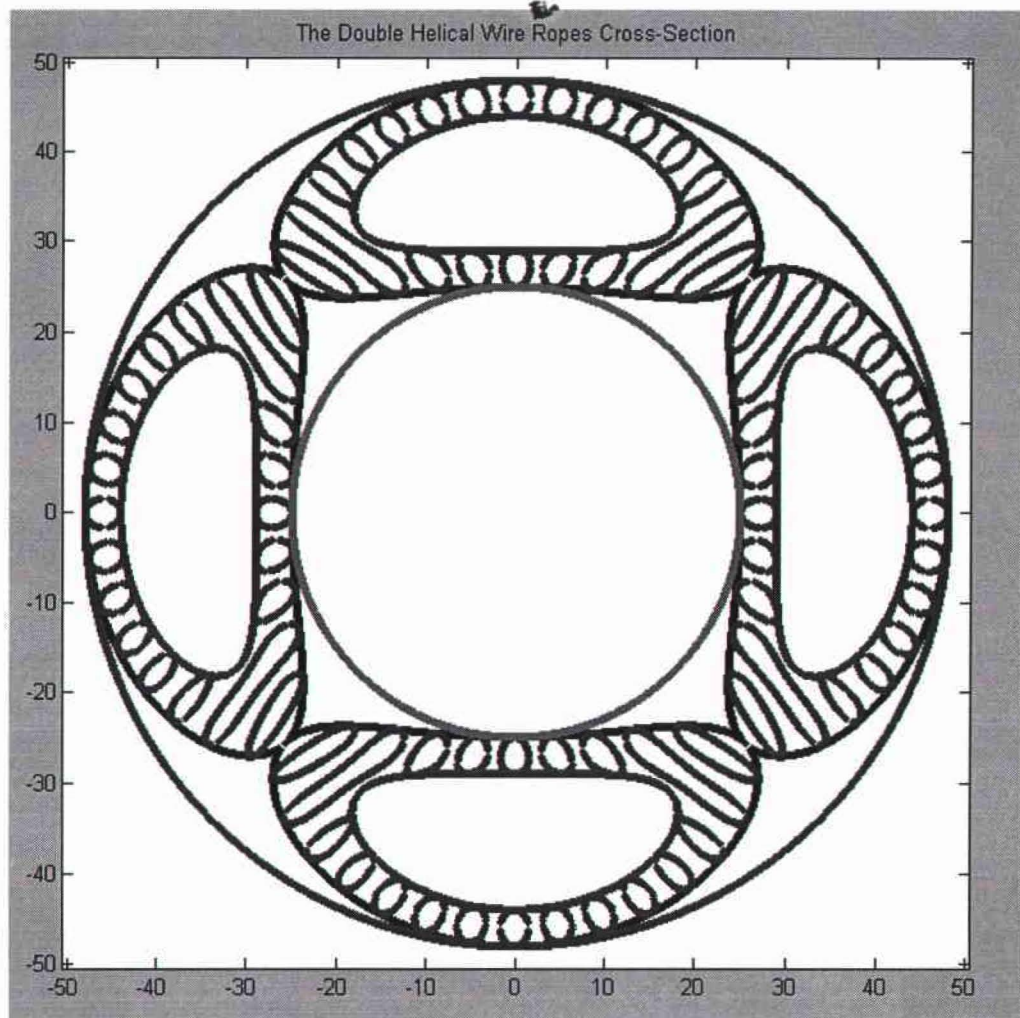


Figure 6-4 Double helical wire rod cross-section with two helix angles having opposite direction

Figure 6-5 shows both possible transverse cross-sections of a double helical wire rods with the dimensions, wire number and strand number described in the above paragraphs. In the figure can be seen both possible shapes in order to compare them and observe the differences produced with both models.

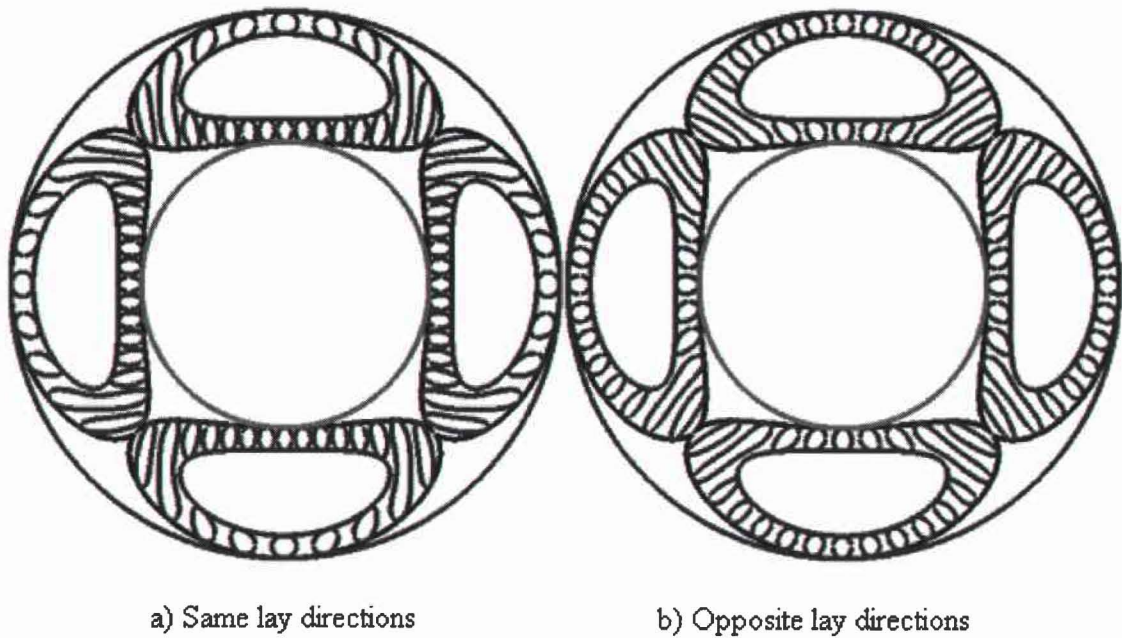


Figure 6-5 The two possible cross-section for a double helical wire rod with some physical characteristic

Figure 6-6 shows a picture of the double helix cable designed with larger diameter components. Due to the elasticity of the materials used (polyurethane) and the larger diameter as well, it did not result in this model and it unrolled once left aside (without the torque that maintained its position fixed). Due to the complexity in the manufacturing of a double helix cable with large helix angles, and after several attempts (taking into consideration the materials, machine and human resource costs), finally choose one sample that includes both cases together with wire diameter and central core strand of a lesser gauge. In the physical sample polyurethane was used for the rolled materials and rigid plastic for the central core.

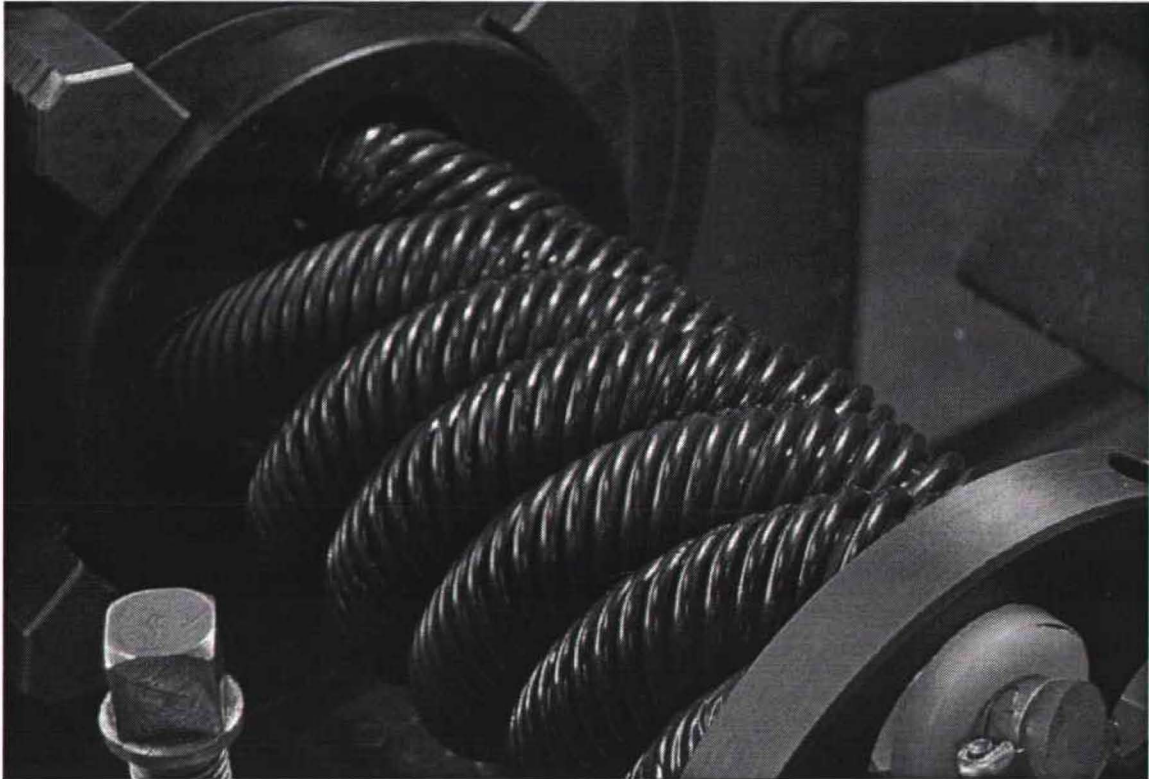


Figure 6-6 Physical model for a double helical wire rod

Figure 6-7 shows a picture of a transverse cross-section of the double helical wire rods designed to compare it with the results obtained by means of the computer algorithm. In the figure, the upper and lower strands correspond to the case where the helix angles are in the same direction and the right and left strands correspond to the case where the first and second helix angles have opposite directions. It is important to highlight the complexity in the construction of a double helix cable used in the physical sample. The mathematical model returns an exact blueprint of the transverse section. In the physical sample it is almost impossible to obtain a symmetric shape due to distortions in the manufacturing process.

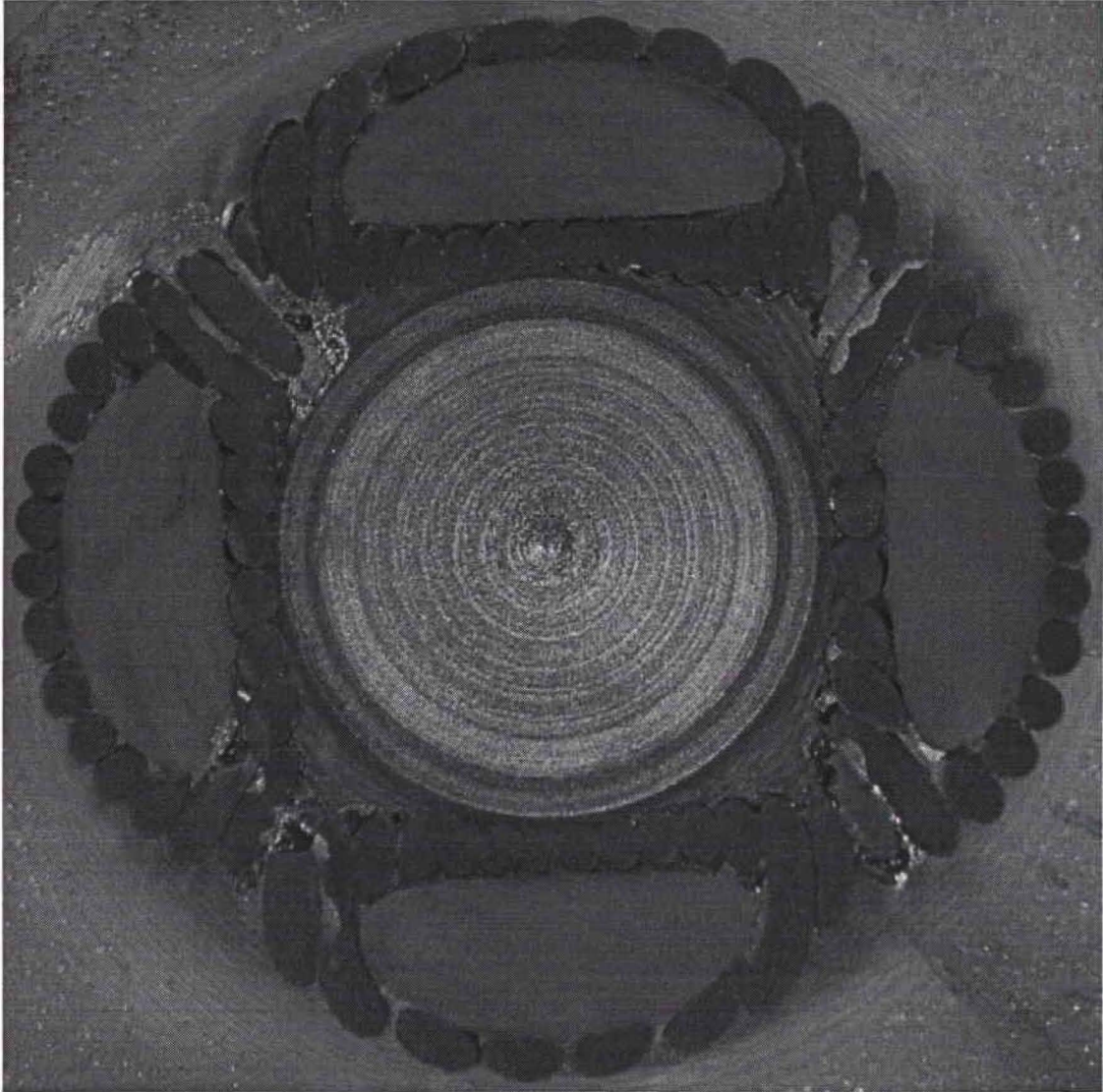


Figure 6-7 Cross-section of a physical model

Also is important to highlight that the transverse cross-section of a double helix cable has infinite shapes that depends on the initial and final position of the wires that conform the strands. The different shapes that the transverse cross-section of a double helical wire rod can have are greatly exaggerated when the helix angles and the wire diameters are large. This phenomenon is graphically explained in the following paragraph.

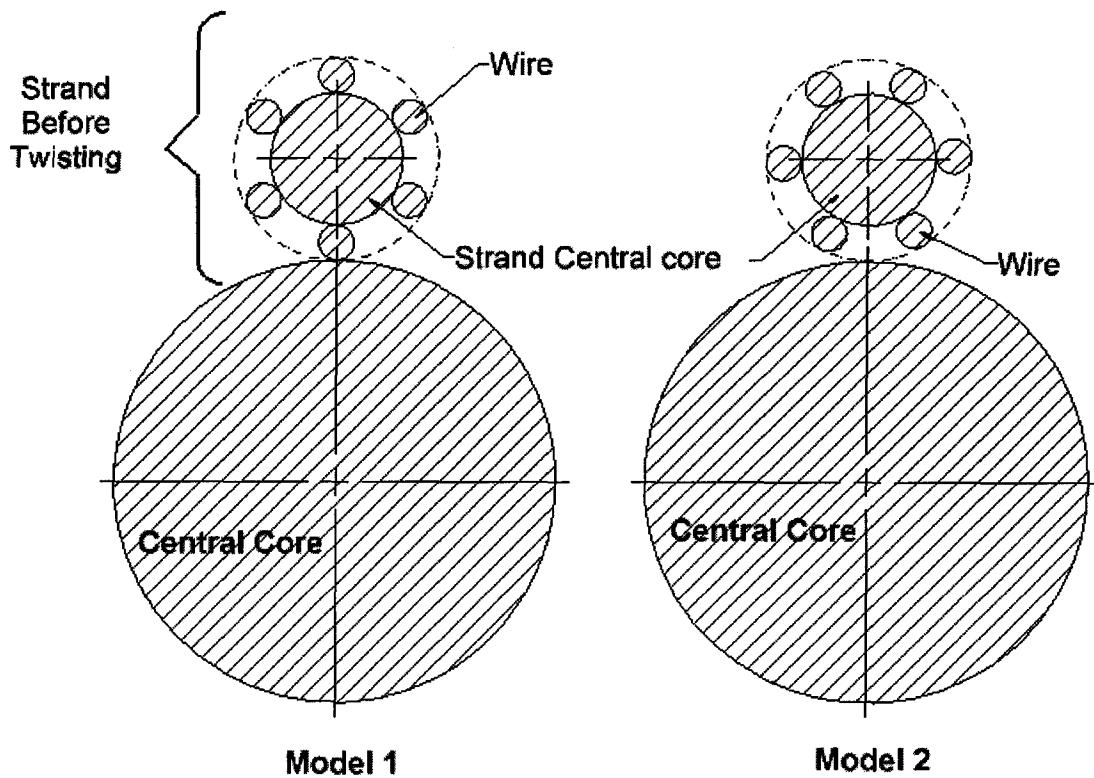


Figure 6-8 Two models with same physical characteristic but with wire's center in different positions

Figure 6-8 shows two double helical wire rods with identical physical characteristics, but the initial position of the wires in the strands are different. The mathematical model developed in this investigation was based on Model 1 in figure 6-8; hence other way would have been more difficult. The same criteria were followed for the determination of the x-y plane, hence $z = 0$ was used. If we consider that theoretically the wire and strand centers should maintain their positions after each turn, evidently the final shapes are infinite and dependant on these positions.

CHAPTER 7

CONCLUSIONS

The main challenging goal in this thesis was successfully achieved: Develop a mathematical algorithm able to describe the transverse section of a double helix cable.

The developed model in this investigation can describe exactly the transverse section of a double helix cable, even if the double helix cable has both angles (first and second helix), in same or opposite directions. A double helix cable may have two possible transverse cross-sections if the components have the same dimensions. These two possible forms depend on the direction of the first and second helix. When both angles have the same direction, the resulting shape is completely different to the one when the helix angles have opposite directions. This model can be used for any case where the transverse section of the components of a double helix, can be drawn with regard to the distribution of the center of the double helix cables in the transverse plane.

The model can be applied in a practical way to determine the interstitial gaps needed to be filled with water-blocking materials. This is a key point since in the cable industry, knowing in advance the transverse geometry of the double helical wire rods, production can be planned accurately, hence saving important costs from a logistics standpoint, since will be known exactly the raw materials needed for specific productions.

The key point in this investigation was the mathematical equations derived that describe the helical path of the second helix. With this path, the second important step was using the “Pencil of Spheres” equation together with the helical path. Finally, deriving this equation, representing the envelope of the “Pencil of Spheres”, intercepted

with the $z=0$ plane, the transverse section of a double helix cable for each wire that forms the double helical wire rods is obtained.

REFERENCES

Wilson, C. E, Sadler J. P. and Michels W. J., 1983, "Kinematics and Dynamics of Machinery", Harper and Row, Publishers, New York p.p. 319-323.

Knapp, R. H., 1988, "Helical Wire Stresses in Bent Cables", Department of Mechanical Engineering, University of Hawaii at Manoa, Honolulu, Hawaii.

Kunoh, T. and Leech C. M., 1985, "Curvature Effects on Contact Position of Wire Strands", Department of Mechanical Engineering, University of Manchester U.K.

Boltyanskii, V. G., 1964, "Envelopes", The Macmillan Company New York.

Etter, D. M., 1993, "Engineering Problem Solving with MATLAB", Prentice Hall, Englewood Cliffs, New Jersey